5-8-2015

Influence of Intracellular Nitrogen Status and Dynamic Control of Central Metabolism in the Plant Symbiont Sinorhizobium meliloti

Reed A. Goodwin
University of Connecticut - Storrs, goodwinr@stanford.edu

Influence of Nitrogen Status and Dynamic Control of Central Metabolism in the Plant Symbiont *Sinorhizobium meliloti*

Reed A. Goodwin, PhD

University of Connecticut, 2015

Sinorhizobium meliloti is a soil bacterium capable of forming an intracellular symbiosis with temperate legumes. During symbiosis *S. meliloti* will fix atmospheric nitrogen, which it provides to its host plant. In return for fixed nitrogen, the plant provides its microsymbiont with carbon in the form of C_4-dicarboxylates. While most well studied model organisms preferentially use glucose as a carbon source, *S. meliloti* prioritizes succinate. During growth on succinate, *S. meliloti* will repress operons dedicated to catabolism of secondary carbon sources, a phenomenon referred to as succinate-mediated catabolite repression (SMCR). SMCR is controlled by an incomplete phosphotransferase system (PTS), which, unlike carbohydrate-type PTS, is a regulatory system that is not involved in sugar transport. This work uses a biochemical approach to elucidate the signals involved in regulating PTS activity.

Biochemical characterization of *S. meliloti* EI^{Ntr} revealed that the enzyme is inhibited by glutamine, a major signal of nitrogen availability in proteobacteria. EI^{Ntr} detects glutamine through its N-terminal GAF domain, a ubiquitous small molecule binding domain. In contrast to *E. coli* EI^{Ntr}, the *S. meliloti* enzyme is not activated by α-ketoglutarate. The differences in EI^{Ntr} regulation likely reflect the preferred carbon source of each organism, with glucose entering central metabolism through glycolysis and

succinate entering through the TCA cycle, sharing a metabolic pathway with α-ketoglutarate. Phosphorylated HPr-His in *S. meliloti* is much less stable than *E. coli* P~His-HPr, and this instability is due to an arginine residue that is conserved within α-proteobacteria that only contain an incomplete PTS. Rapid phosphohydrolysis of P~His-HPr in the α-proteobacteria may be act to remove phosphate from the system to avoid oversaturation, a problem that is not faced by sugar-phosphorylating PTS. The work presented here sheds light on how the PTS of *S. meliloti* integrates carbon, nitrogen, and energy levels within the cell in order to regulate SMCR.

Influence of Intracellular Nitrogen Status and Dynamic Control of Central Metabolism in the Plant Symbiont *Sinorhizobium meliloti*

Reed A. Goodwin

B.S., Washington State University, 2007

A Dissertation

Submitted in Partial Fulfillment of the

Requirements for the Degree of

Doctor of Philosophy

at the

University of Connecticut

2015

APPROVAL PAGE

Doctor of Philosophy Dissertation

Influence of Intracellular Nitrogen Status and Dynamic Control of Central Metabolism in the Plant Symbiont *Sinorhizobium meliloti*

Presented by

Reed A. Goodwin, B.S.

Major Advisor _____

Daniel J. Gage

Associate Advisor _____

Victoria Robinson

Associate Advisor _____

David Benson

Associate Advisor _____

Joerg Graf

Associate Advisor _____

Carolyn Teschke

Associate Advisor _____

Kenneth Noll

University of Connecticut
2015

Acknowledgements

I would like to thank my advisor, Dr. Dan Gage, who was a great mentor during my time in grad school. I could not have asked for a better advisor. I'd like to thank my committee, Drs. David Benson, Joerg Graf, Carol Teschke, Ken Noll, and especially Vikki Robinson. Vikki not only gave me access to the equipment in her lab, but also gave me advice whenever I needed it.

I'd like to thank my dad, who has been incredibly supportive of my time in grad school, and Misha, my wonderful sister. The rare occasions I get to visit the two of you are always the best parts of my year, and I wish I had visited more often. To my grandmother, the most unfailingly happy person I know, you are the center of our family.

I am indebted to everyone I have shared the lab with, both past and present. Life is never dull working with Jamie, Charles, and Michael. My former lab mates Preston, Cata, and Emma, who have all helped me through my journey. I want to thank Sarah, for all the support over the last 9 months. It would have been a lot more difficult to get through this final stretch without you. Lindsey, my neighbor both at work and at home, when I was new to Connecticut and had nobody to celebrate the holidays with you made me a part of your family, and I am incredibly grateful for that. Last, but definitely not least, I must acknowledge Andrew Collins, my roommate of five years and my best friend. I don't know that I would have made it through grad school without having such a great friend to spend time with after work every day.

Table of Contents

List of Figures

Chapter 1
Introduction

The importance of nitrogen in agriculture. Nitrogen availability is critical in both natural ecosystems as well as crop production (1). While abiotic processes such as lightning fix a limited amount of nitrogen (<10 Tg yr^{-1}), biological nitrogen fixation (BNF) is responsible for the majority of non-industrial nitrogen fixation (2). Currently, anthropogenic nitrogen fixation contributes approximately 210 Tg of the 413 Tg yr^{-1} fixed globally (3). With a global population of approximately 7 billion people that is rapidly growing, the demand for food will increase greatly during the approaching decades (4). As food production increases so too will the fertilizer production required to support the growth of crops. Currently, artificial production of nitrogen fertilizer is accomplished through the Haber-Bosch process, which feeds approximately half of the world's population (5). Despite improvements since its development, the Haber-Bosch process requires considerable amounts of energy, consuming 54 MJ kg^{-1} N and generating 1.4 kg CO_2 kg^{-1} nitrogen (6). It is clear that with increasing concerns regarding global warming and energy supplies alternative means of nitrogen fertilization must be developed.

Humans began domesticating both plants and animals about 10,000 years ago in the fertile cradles of civilization. Early in the process it was recognized that the application of manure supported crop growth, though the reason for this was not understood (7). The Romans discovered that intermingling legumes within their staple crops led to increased yields, though once again the reason for this was not understood. It

was not until 1836 that Jean-Baptiste Boussingault discovered that the growth of leguminous plants increased the availability of nitrogen (7). While this concept was not accepted initially, experiments performed by Hellriegel and Wilfarth led to a general acceptance of this concept (8). Not only did they show that legumes were increasing soil nitrogen levels, but this only happened in plants that had bacteria-rich nodules on their roots.

Sinorhizobium meliloti. The α-proteobacterium *Sinorhizobium meliloti* is capable of nitrogen fixation during symbiosis with a narrow range of legumes belonging to genera such as *Medicago*, *Melilotus*, and *Trigonella* (9, 10). Members of the Rhizobiaceae that are closely related to *S. meliloti* include plant symbionts in the *Rhizobium* genus, plant pathogenic *Agrobacterium* spp. and animal pathogenic *Brucella* spp. (11). The genome of *S. meliloti* strain Rm1021 is tripartite, with one primary chromosome (3.65 Mb) and two symbiotic megaplasmids pSymA and pSymB (1.35 Mb and 1.68 Mb, respectively) (12). Complex, multipartite genomes are common features within the *Rhizobiaceae*, and are intimately linked with eukaryotic host interactions (13). *S. meliloti* has the capacity to catabolize a wide range of carbon substrates (14). When the genome was sequenced it was reported that there were a large number of genes involved in solute transport, comprising 12% of the overall genome and are particularly abundant on pSymB (17.4% of genes present on the megaplasmid) (12).

Rhizobia-legume symbiosis. Rhizobia is a term traditionally used for nitrogen fixing, plant symbiotic α-proteobacteria belonging to the genera *Azorhizobium*, *Bradyrhizobium*, *Mesorhizobium*, *Rhizobium*, and *Sinorhizobium* (15). Nitrogen fixation in rhizobia occurs only during symbiosis with a suitable host. In a majority of the rhizobia-legume

symbioses the bacteria will invade plant roots and become enclosed in a symbiosis-specific organ called the root nodule (16). The root nodule is critical for maintaining the precise conditions required to support nitrogen fixation, such as maintaining a reduced oxygen tension and feeding the bacteria the carbon required to maintain the energetically costly reduction of molecular nitrogen (17, 18). Depending on the plant host, nodules can be indeterminate, which means they have a persistent meristem that is continually infected by new rhizobia, or determinate, which undergo a predetermined growth program, and lack the meristem required to continually generate new nodule tissue (16). Due to these characteristics, indeterminate nodules predominantly appear elongated, whereas determinate nodules are rounded in shape. There is a wide variety of host species that rhizobia will nodulate and the range is specific to the bacterial species. Some rhizobia are highly promiscuous, such as *Sinorhizobium fredii* NGR234 and *S. fredii* USDA257, which can nodulate 232 and 135 different legume species (112 and 79 genera), respectively (19). In contrast, rhizobia such as *S. meliloti* have narrow host-ranges that span few genera. Differences in host ranges occur due to factors inherent to both the plant and its symbiont. Successful nodulation depends on the ability of plants to elicit bacterial responses using secreted signals, detection by the plant of lipochitooligosaccharides called Nod factors (see below), production of exopolysaccharides by the bacteria, and resistance of the bacterium to nodule-specific cysteine-rich (NCR) peptides (10, 20-22).

***S. meliloti-Medicago* interactions in the soil.** A plant's rhizosphere is a complex ecosystem containing great diversity both in terms of the life present and their interactions (23). Plants exude a considerable amount of nutrients, allowing them to mold

their communities (24-26). Rhizosphere bacteria must compete with each other for available nutrients and space, as well as survive predation by protozoa (27-29). Many plants nurture communities of beneficial bacteria that protect the plant from pathogens and participate in resource exchange. Rhizosphere constituents, such as *Pseudomonas fluorescens,* produce a wide array of antimicrobial compounds that can restrict the proliferation of parasitic organsims (26). These interactions are further complicated by abiotic factors such as soil structure and pH, osmotic stress, and mineral composition (30-33). The rhizosphere community can compete with host plants for nutrients such as nitrogen and is critical for the cycling of this element through the environment (34). While many rhizobia will chemotact towards plant exudates their actual mobility within soil is low (35, 36).

S. meliloti has evolved to not only thrive within the rhizosphere, but to form an intracellular symbiosis within certain plants (16). The formation of this symbiosis is very complex, requiring communication between host and symbiont as well as multiple signal cascades within each organism. The host plant is seen as being in control of the symbiosis, only initiating the relationship during times of nitrogen limitation, and only allowing it to continue while its symbionts remain productive (37-39). If host plants do not receive sufficient fixed nitrogen during symbiosis (either due to non-fixing 'cheaters' or environmental inhibition) they will sanction their symbionts by cutting off the oxygen supply to the nodule (40, 41).

Establishment of symbiosis by *S. meliloti.* The three NodD proteins of *S. meliloti* are constitutively expressed transcriptional regulators. NodD1 and NodD2 sense flavonoids produced by host plants and in response will activate transcription of the *nod* genes,

which are responsible for synthesis of Nod factor (42). Nod factors, perhaps the best studied specificity determinant, are composed of N-acetylglucosamine backbones that have an acyl group attached to the non-reducing end and various modifications of the backbone (43). The exact structure of Nod factors depends on the species producing them, and specificity is determined by characteristics such as: backbone length, acyl group saturation, and decoration of the terminal sugars (44). The most common substitutions at the non-reducing end are methyl, acetyl, and carbamoyl groups, while fucosyl, acetyl, and sulfate groups are found on the reducing end (45). Recognition of Nod factors by the plant is mediated by LysM-like receptor kinases (43). Host compatibility can be modified by production of exotic Nod factors by a symbiont or expression of heterologous Nod factor receptors in the plant.

Perception of Nod factor by the plant triggers a series of responses, including calcium oscillations (Ca^{2+} spiking), actin rearrangement, and membrane depolarization, all of which lead to curling of the root hair (16). Invasion of the host plant begins when Nod factor dependent deformation of the root hair traps a colony of *S. meliloti* in a structure called the shepherd's crook. Within the shepherd's crook a section of the cell wall will invaginate due to localized degradation of the cell wall, forming a tube that grows down the length of the root hair (46). This tube, called an infection thread, grows through localized deposition of cell wall material. Bacteria within the infection thread grow downwards, following its progress down the root hair in columns one to two bacteria wide (47). Growth down the root hair is largely clonal, with only a few ancestral cells giving rise to the population invading the plant. Inoculation experiments with mixed populations of isogenic strains expressing GFP or RFP reveal sectored infection threads,

with discreet bands of each strain. In indeterminate plants continued growth of the infection thread depends on production of symbiotically active exopolysaccharides produced by the invading bacteria. In the case of *S. meliloti*, strains incapable of producing either EPS I (succinoglycan) or EPS II (galactoglucan) form bloated infection threads that prematurely terminate (48). The precise role of these EPS is not known, though they appear to be related to signaling since exogenous application of picomols of EPS will restore infectivity of *exo* mutants. When the infection thread reaches the basolateral epidermal cell wall it will fuse with the wall, releasing bacteria into the intracellular space. At this point the infection thread will fragment as cells move through threads forming in cortical cells (49). As the infection thread develops, cells of the inner-cortex will resume cell division and develop into a mass that will become the nodule primordium. Once the bacteria reach the nodule primordium they will be endocytosed in membrane-bound vesicles called the symbiosome. Within the symbiosome NCR peptides will trigger terminal differentiation of the bacteria into branched cells with endoduplicated chromosomes called bacteroids (50). It is the bacteroids within the symbiosomes that carry out nitrogen fixation.

Metabolism within the nodule. Differentiation into bacteroids involves significant rearrangement of a cell's metabolism in order to support nitrogen fixation. Bacteroids face a unique challenge in that nitrogenase is oxygen-labile, but rhizobia are obligate aerobes that require oxygen for energy production. The host plant provides a solution to this problem by maintaining an oxygen tension that is high enough to maintain metabolism without exceeding levels that would deactivate the nitrogenase. The three main mechanisms used to reduce the oxygen concentration within nodules are a diffusion

barrier created by the dense nodule tissue, consumption of O_2 due to respiration of both plant mitochondria and bacteroids, and expression of leghemoglobins by the plant. Leghemoglobins are oxygen-binding proteins that lend effective nodules their pink hue. When the symbiotic leghemoglobins of *Lotus japonicus* grown in nitrogen-limiting conditions are knocked down using RNAi, the plants become stunted and leaves chlorotic, despite nodulation with *Mesorhizobium loti* (51). The oxygen gradient in nodules of LbRNAi strains is very shallow, and does not decrease below 4.5% of atmospheric levels at the center. These strains also have ATP:ADP ratios that are only 20% of wild-type, while the total adenylate pool was not significantly different. It has been proposed that the difference indicates an important role for leghemoglobins in maintaining respiration rates within the nodule. In order to cope with the low oxygen levels in nodules the bacteroids switch to a cbb_3 type cytochrome oxidase (encoded by *fixNOQP*), which has a very high affinity for O_2 (52).

In return for fixed nitrogen the plant will provide bacteroids with a steady flow of C_4-dicarboxylic acids such as succinate, malate, and fumarate. *S. meliloti* DctA, a member of the major facilitator superfamily, is the primary protein responsible for uptake of dicarboxylates. Mutation of the *dctA* gene results in strains that can nodulate legume hosts, but are unable to fix nitrogen (53). Due to the lack of nitrogen fixation, nodules formed by *dctA* mutants senesce early. In free-living conditions, transcription of *dctA* is dependent on the two-component system formed by DctBD (54). DctB is a membrane-bound histidine kinase with a periplasmic ligand binding domain and a cytoplasmic kinase domain. When DctB binds dicarboxylate ligands it will phosphorylate the response regulator DctD. In turn, phosphorylated DctD activates σ^{54}-dependent

transcription of *dctA*. While DctA is required for nitrogen fixation, *dctB* and *dctD* are dispensable, which indicates that expression of *dctA* within the nodule is dependent on an as yet unknown system.

In order to grow using TCA cycle intermediates as the sole carbon source bacteria need an intact gluconeogenic pathway. In many bacteria, including rhizobia, a major early step in gluconeogenesis is the conversion of oxaloacetate to phosphoenolpyruvate (PEP) catalyzed by PEP carboxykinase (Pck, encoded by *pckA*) (55). In many rhizobia mutation of *pckA* abolishes growth on TCA cycle intermediates. In *S. meliloti*, *pckA* mutants are able to grow very slowly on dicarboxylates due to the combined activity of pyruvate orthophosphate dikinase (PPDK) and the NAD^+-dependent malic enzyme (encoded by *dme*) (56). Bacteroids inoculated with *pckA* mutants reduce acetylene at 60% of the rate of wild-type *S. meliloti,* despite the fact that Pck activity is undetectable within the nodule (57). It is believed that bacteroids, unlike free-living cells, replenish acetyl-CoA using the malic enzyme as opposed to Pck (57-59). Gluconeogenesis mutants that lack detectable enolase, glyceraldehyde-3-phosphate dehydrogenase, or 3-phosphoglycerate kinase activity form small, white, Fix^- nodules (57). A major difference between bacteria in symbiosis with determinate and indeterminate nodules is accumulation of poly-β-hydroxybutyrate (PHB). Symbionts of plants that form determinate nodules will begin accumulating PHB during the first steps of symbiosis and the PHB granules will persist throughout the relationship (60). While bacteria infecting plants that form indeterminate nodules will also accumulate PHB during the initial stages of invasion the granules will disappear before differentiation into bacteroid states (61). While genes for PHB degredation are dispensable for these bacteria they must have intact

PHB synthesis pathways in order to establish a proper symbiosis. This is generally interpreted as a method for balancing the intracellular redox state as opposed to storage of excess carbon.

Plant-bacteroid nitrogen exchange. It's not clear exactly how nitrogen is exchanged between bacteroids and host plants. It has been proposed, based on two lines of evidence from *R. etli*, that the fixed nitrogen is immediately delivered to the plant either as NH_3 diffusing across the membrane, or NH_4^+ being exported into the peribacteroid space (62). The first line of evidence supporting this is based on the fact that expression of the *E. coli* assimilatory glutamate dehydrogenase (GDH) during symbiosis resulted in severely reduced nodule numbers. This could be due to assimilation of fixed nitrogen by GDH before it could be transferred to the host plant, resulting in an ineffective symbiosis. The second line of evidence came from experiments where the high-affinity ammonium transporter AmtB, which is normally not produced within the nodule, was expressed from the *nifHc* promoter. The ectopic expression of *amtB* resulted in small, white nodules with nearly undetectable nitrogen fixation activity. In this case it was proposed that the bacteroids were competing with the host cells for any ammonium released into the peribacteroid space. These experiments were performed with *Phaseolus vulgaris*, which forms determinate nodules. To determine if the same was true for plants forming indeterminate nodules the work was repeated for the host-symbiont pair of *Rhizobium leguminosarum* and *Vicia hirsuta*. Inappropriate expression of AmtB from the *nifHc* promoter caused the same effect in this system. Further supporting this model is the high activity of ammonium assimilation enzymes, such as glutamine synthetase and glutamate synthase (GS and GOGAT, respectively), within infected cells (63, 64).

Molecular biology of nitrogen fixation. Despite the fact that all life on Earth needs nitrogen BNF has only been shown to occur in prokaryotes called diazotrophs (65). Due to the stability of molecular nitrogen, the most abundant form of the element, BNF is an energy intensive process that requires a very specific set of closely related enzymes called nitrogenases. Regulation of nitrogenase expression differs between diazotrophic organisms. In *S. meliloti*, the regulatory cascade leading to nitrogenase production begins with the membrane-bound histidine kinase FixL (66). FixL autophosphorylates at low oxygen concentrations and phosphorylates the response regulator FixJ. Phosphorylated FixJ induces more than 100 genes, including the transcriptional activator *nifA* (67). NifA belongs to the enhancer-binding protein (EBP) family and stimulates σ^{54}-dependent transcription of the nitrogenase structural genes (68).

Nitrogenases require iron for their activity, and they are subdivided based on their requirement for an additional cofactor: Nif require molybdenum, Vnf require vanadium, while Anf nitrogenases do not require any other cofactor (69). The MoFe Nif nitrogenases are the most extensively studied and will be the focus of this section. The general reaction catalyzed by the MoFe nitrogenase is summarized as:

$$N_2 + 8e^- + 16ATP + 8H^+ \rightarrow 2NH_3 + H_2 + 16ADP + 16P_i$$

The nitrogenase holoenzyme is composed of the structural proteins NifH, NifD, and NifK. The complex is comprised of the Fe protein (a homodimer of NifH) and the MoFe protein (an $\alpha_2\beta_2$ heterotetramer containing two units each of NifDK). The Fe protein contains a 4Fe-4S cluster, while the FeMo protein contains a P-cluster (8Fe-7S), and an M cluster (FeMo-co, 7Fe-Mo-9S-homocitrate) (70).

The role of the Fe protein is to transfer electrons to the MoFe proteins in the Fe protein cycle. After binding two molecules of MgATP the Fe protein associates with the MoFe protein. Both molecules of ATP are hydrolyzed to ADP, which is coupled to the transfer of a single electron and a single proton from the Fe-S cluster to the P-cluster of the MoFe protein. The $NifH_2$-2MgADP complex dissociates, ATP replaces ADP, and the Fe cluster is reduced back to the 1^+ oxidation state. After each electron transfer the P-cluster will pass the electron to the M-cluster. The FeMo protein does not bind N_2 until either three or four electrons have accumulated on the FeMo-co. The N_2 is reduced to two molecules of NH_3 with the subsequent accumulation of the remaining electrons and one molecule of H_2 is evolved during the cycle.

Regulation of central metabolism. Proper coordination of central metabolism is a fundamental challenge for cells. It is critical for an organism's survival to establish a balanced pool of metabolic intermediates, and therefore a cell must modulate the flux required to maintain said pools. In humans, imbalances in pathways such as the TCA cycle have been implicated in the progression of cancer (71), aging (72), response to viral infections (73), obesity (74), and intestinal function (75). Furthermore, control of central metabolism in microbes has garnered significant interest due to its role in pathogenesis (76, 77), antimicrobial resistance (78), metabolic engineering (79, 80), wine production (81), and symbiosis (82, 83). While regulation of metabolism is a process shared by diverse organisms, the underlying molecular mechanisms are highly diverse.

For many bacteria, the response to the composition of carbon encountered in the environment is genetically coded. Carbon catabolite repression (CCR) is a general phenomenon wherein the presence of a preferred carbon source will cause a cell to

actively repress expression of the proteins required for consumption of alternative catabolites. First observed in fungi by Emile Duclaux in 1899 (84), this phenomenon was studied sporadically throughout the first half of the 20th century until Jacques Monod's description of diauxic growth in the 1940's led to unification of the field. Diauxic growth is observed when bacteria are grown in media containing a both a preferred, or primary, carbon source and a non-preferred, or secondary, carbon source. A diauxic growth curve will contain a biphasic exponential phase with two different growth rates separated by a second (diauxic) lag. During diauxic growth an organism will exclusively use the preferred carbon source during the initial exponential phase, enter the diauxic lag once this has been exhausted, then consume the secondary carbon source during the second exponential growth phase. The length of the diauxic lag will depend on the sugar combination used, with contributions from both preferred and non-preferred carbon.

The phosphotransferase system (PTS). The PTS was first detected as a sugar-transport/phosphorylation system in extracts of *E. coli* in 1964 and was later found to be a global regulator of CCR (85, 86). This system is comprised of two general proteins, EI and HPr, as well as the sugar-specific Enzyme II (87). EII are divided into the A, B, C, and occasionally D domains that can either be isolated proteins, or fusions among the different domains. EIIA and EIIB are cytoplasmic proteins, while EIIC is the transmembrane protein responsible for sugar uptake (88). EI initiates the phospho-transfer cascade by autophosphorylating using PEP as a substrate (89). The phosphate is transferred sequentially onto an invariant histidine in HPr, then onto EIIA (85). Enzyme IIA can pass this phosphate onto EIIB, which phosphorylates sugars being transported by EIIC. In *E. coli*, EIIA^{Glc} is the central player in controlling CCR. EII^{Glc} is comprised of

the cytoplasmic $EIIA^{Glc}$ and the membrane associated $EIICB^{Glc}$ (the order written corresponds to the domain order in the expressed protein). During growth on glucose $EIIA^{Glc}$ will exist primarily in its dephospho form, which binds transporters for secondary carbon sources and locks them in an inactive state (90). Deactivating sugar uptake systems prevents activation of their catabolic operons, a phenomenon called inducer exclusion. As glucose is depleted from the environment $P\sim EIIA^{Glc}$ will become the predominant form. Phosphorylated $EIIA^{Glc}$ has a low affinity for secondary sugar transporters and stimulates adenylate cyclase activity. As cAMP levels rise in the cell it complexes with the cAMP receptor protein (CRP), which activates transcription of secondary catabolite operons.

The PTS of many Firmicutes, such as *Bacillus subtilis*, is structurally similar, but mechanistically different than the enteric PTS. In addition to the proteins present in the enteric system the Firmicutes contain an ATP-dependent HPr kinase/phosphorylase (HPrK/P), which phosphorylates HPr on a conserved serine (91). In this case it is not $EIIA^{Glc}$, but P-Ser-HPr that regulates CCR. When HPr-Ser is phosphorylated it gains the ability to bind the catabolite control protein A (CcpA), and the resulting complex is able to bind regulatory DNA sequences called catabolite response elements (*cre*) (92). Binding of this complex to a *cre* will alter the expression of the downstream gene depending on whether it binds upsteam (increased expression) or downstream (decreased expression) of the promoter sequence. Like $EIIA^{Glc}$ of enteric bacteria, the P-Ser-HPr of Firmicutes mediates inducer exclusion in the presence of a preferred carbon source in a CcpA-independent manner.

Phosphorylation of HPr-Ser by HPrK in many low G+C Gram-positive bacteria is stimulated to varying degrees by fructose-1,6-bisphosphate (a major signal of glycolytic flux) (93). HPrK dependent phosphorylation of HPr is bidirectional, and HPr-Ser-P can be removed using inorganic phosphate as a substrate, generating pyrophosphate. The pyrophosphate generated by this reaction can in turn be used by HPrK to re-phosphorylate HPr-Ser.

Variations of the PTS. As complete genome sequences from a wide range of bacteria were published it became obvious that the distribution of PTS proteins was more diverse than originally believed (94). Two of the most common deviations from the canonical PTS are the so-called incomplete PTS, which lack EIIBC, and multiphosphoryl transfer proteins (MTPs), which are fusions of EI, HPr, and EIIA into a single polypeptide. In bacteria with incomplete PTS, which contain an EI, HPr and one or more EIIA(s), the system is assumed to fulfill a regulatory function. In *E. coli*, there is an incomplete PTS parallel to the carbohydrate system that has been termed the PTS^{Ntr}, which is comprised of EI^{Ntr}, NPr, and $EIIA^{Ntr}$ (95). The Ntr refers to nitrogen, and the name originates from the fact that *ptsO* and *ptsN* (the genes that encode NPr and $EIIA^{Ntr}$, respectively) are found within an operon with the *rpoN* gene, which encodes the nitrogen-stress related σ^{54}. Additionally, many proteobacteria with incomplete PTS often possess an HPrK, which is a protein traditionally associated with only low G+C Gram-positive bacteria (87, 94). While EI^{Ntr} largely resembles its carbohydrate-type counterpart it has an additional N-terminal GAF domain, the importance of which will be discussed below. The gene encoding EI^{Ntr} (*ptsP*) has only been found in the proteobacteria, while *ptsN* is present in some spirochetes and chlamydiae (94).

Incomplete PTS have been shown to regulate a wide variety of behaviors, most of which are related to central metabolism. In most cases it appears to be dephospho-EIIA that physically interacts with the associated proteins. $EIIA^{Ntr}$ have been shown to interact with two-component systems, ABC transporters, and metabolic enzymes. The *E. coli* PTS^{Ntr} controls intracellular potassium levels, the phosphorous stress response, and TCA cycle flux. It has been shown that $EIIA^{Ntr}$ regulates potassium homeostasis through direct interaction with TrkA, a subunit of the low-affinity potassium transporter, and KdpD, the histidine kinase of the potassium stress two-component system (96, 97). In regulating these two systems $EIIA^{Ntr}$ is not only controlling potassium uptake, but also selectivity of RNA polymerase for σ^{70} and σ^{S} (98). $EIIA^{Ntr}$ participates in the phosphate stress response through interaction with the PhoR/PhoB two-component system (99). When $EIIA^{Ntr}$ binds PhoR it stimulates phosphorylation of PhoB, which in turn alters the expression of genes involved in phosphate assimilation. Metabolome studies on a *ptsN* strain of *E. coli* revealed an increase in acetate excretion during growth, accompanied by a decrease in carbon flux into the TCA cycle (100). The authors found that during growth on glucose many of the genes encoding TCA cycle enzymes were repressed. In *Pseudomonas putida*, which has both a PTS^{Ntr} and PTS^{Fru}, the PTS^{Ntr} controls polyhydroxy alkanoate production and TCA cycle flux. The *Ralstonia eutropha* incomplete PTS (parallel to a PTS^{Nag}) is comprised of a carbohydrate-type EI, HPr, HPrK and $EIIA^{Ntr}$. Deletion of *hprK* is lethal, but the effect is epistatic with *hpr*, meaning the gene could be deleted in Δ*hpr* backgrounds. Expression vectors containing three *hpr* alleles were conjugated into the double mutant. Plasmids expressing wild-type HPr and HPr(S46A) were transferred at nearly undetectable rates, while transconjugants

expressing HPr(H15A) were frequently isolated (albeit at a rate 200-fold below the empty vector). Ligand fishing and bacterial two-hybrid assays demonstrated that dephospho-EIIA^{Ntr} could bind the ppGpp synthase/hydrolase SpoT1 (101).

Carbon catabolite repression in *S. meliloti.* CCR was first observed in *S. meliloti* almost 40 years ago (102). As opposed to glucose-mediated repression in *E. coli*, *S. meliloti* displays diauxic growth when grown on lactose and limiting amounts of succinate (succinate-mediated catabolite repression; SMCR). The authors also reported that diauxie was observed during growth in combinations of succinate and either maltose or cellobiose. When succinate was present in the growth medium β-galactosidase activity was low whether or not lactose was present. β-galctosidase activity was not increased in the presence of gratuitous inducers isopropyl-β-D-thiogalactopyranoside (IPTG) or thio-methyl-galactopyranoside (TMG) and addition of cAMP did not decrease the succinate-lactose diauxic lag. CCR by TCA cycle intermediates has been shown to occur in other plant and soil-associated bacteria such as *R. leguminosarum, A. vinelandii*, *P. aeruginosa*, and *Azospirillum brasilense* (103-106).

Gage and Long found that expression of *agpA*, the gene encoding an α-galactoside periplasmic binding protein, was repressed by the symbiosis regulator SyrA (107). When the *agpA*::Tn*phoA* strain was grown in medium containing glucose the alkaline phosphatase activity decreased, while the converse was true for media containing α-galactosides such as melibiose. While glucose exerted repression over *agpA* expression it does not manifest in diauxie when *S. meliloti* is grown in limiting glucose and lactose (102). Bringhurst and Gage later found that expression of *agpA* and growth on α-galactosides requires the *agpT* gene, which encodes an AraC-like transcriptional

regulator transcribed divergently from the *agp-melA* operon (108). It was also shown that α-galactoside metabolism is subject to inducer exclusion when succinate is present in the medium (109).

Analysis of the *S. meliloti* genome reveals an incomplete PTS (Fig. 1.2) consisting of EI^{Ntr}, HPr, HPrK, $EIIA^{Ntr}$, and $EIIA^{Man}$ (encoded by the genes *ptsP*, *hpr*, *hprK*, *ptsN*, and *manX*, respectively) (110). The genes *hprK*, *manX*, and *hpr* are clustered in the same orientation on the chromosome, with the reading frames of *manX* and *hpr* overlapping (Fig. 1.1). As in *E. coli*, *ptsN* is located in an operon with the nitrogen-stress related sigma factor gene *rpoN*. Finally, *ptsP* is located between the genes *lysC*, and *prfA*, though each of these genes has a predicted promoter sequence, making it unlikely that they are co-transcribed. Previous genetics experiments have provided a model for how the PTS imposes SMCR in *S. meliloti* (110, 111). According to this model, flux of phosphate from EI^{Ntr} through HPr-His results in an increase in SMCR. Whether it is HPr-His~P, $EIIA^{Ntr}$~P, $EIIA^{Man}$~P, or a combination of all three that imposes SMCR is currently unknown, though it is likely that all three are involved to varying degrees. HPrK phosphorylation of HPr-Ser acts in opposition to this process, presumably by decreasing the rate of HPr phosphorylation by EI^{Ntr}. It is currently unknown how HPrK activity is regulated, but it is possibly stimulated by a metabolic intermediate(s) such as fructose-1,6-bisphosphate and inhibited by P_i like HPrK in *Brucella melitensis* (112). In addition to controlling SMCR, the PTS of *S. meliloti* influences the accumulation of PHB, production of succinoglycan, and nodulation of *M. sativa*.

Global regulation of SMCR in *S. meliloti* also involves the two-component system encoded by the genes *sma0113* and *sma0114* (113). Deletion of *sma0113* caused a

relaxed SMCR phenotype in cells grown in media containing succinate and either lactose, raffinose, or maltose. The protein encoded by *sma0113* is an HWE-histidine kinase containing 5 PAS domains. Relief of SMCR in the *sma0113* background was found to be epistatic with HPr, implying that its role is upstream of the PTS in *S. meliloti*. The downstream gene, *sma0114*, encodes a small CheY-type response regulator protein containing a PFxFATGY motif and lacking the traditional α4-helix (114). While deletion of *sma0114* does not cause relaxed SMCR it does result in an increase in polyhydroxybutyrate (PHB), a phenotype that requires an intact copy of *sma0113* (113).

Purpose of this study

Unlike many of the well-studied bacteria, succinate is the preferred carbon source in *S. meliloti* and its presence results in repression of operons dedicated to catabolism of secondary carbon sources. Like many other bacteria, *S. meliloti* regulates CCR using a phosphotransferase system, although unlike the canonical PTS there are no associated EII transport proteins and succinate is not phosphorylated during uptake. The function of the PTS has broad physiological implications, as highlighted by the severe growth defects exhibited by deletion of the *hprK* gene, which still manifest during growth on succinate. Experiments using genetic and physiological methods indicate that flux of phosphate through HPr-His results in imposition of SMCR. A large gap in our understanding of the PTS includes the mechanism by which PTS activity is controlled. Enzyme I^{Ntr} is the first step in the phosphorylation cascade, and presumably is responsible for regulating the introduction of phosphate into the HPr-His branch of the PTS. In this study a biochemical approach was used to determine the metabolic signals that are detected by EI^{Ntr} and propagated throughout the PTS.

The mechanism by which phosphate is drained from an incomplete PTS is not currently known. While a sugar-specific PTS uses the imported sugar as a natural sink for phosphate, this transport reaction does not occur in incomplete PTS. Dephosphorylation of HPr-Ser-P, which is does not lead to sugar phosphorylation, is generally mediated by the phosphorylase activity of HPrK. In *Mycoplasma pneumoniae,* HPr-Ser-P is dephosphorylated by a PP2C-type phosphatase encoded by the *prpC* gene. To our knowledge enzymatic dephosphorylation of HPr-His~P or EIIA-His~P (excluding the transfer involved in sugar uptake) has not been detected in any system. A possible mechanism is proposed based on a unique sequence characteristic that is conserved within α-proteobacteria that only contain regulatory PTS.

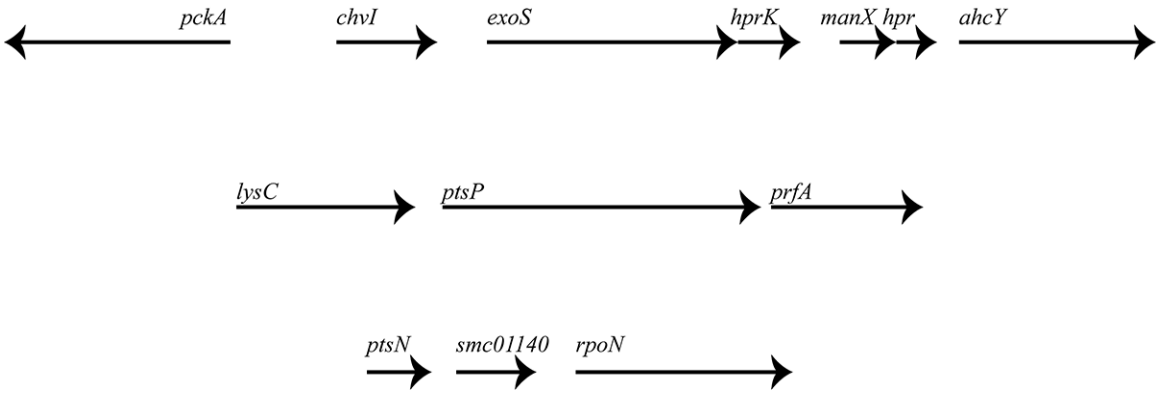

Figure 1.1 PTS gene neighborhoods. Top, *hprK-manX-hpr* locus. This gene order is highly conserved within the rhizobiales. The reading frames of *exoS* and *hprK* overlap, as do *manX* and *hpr*. This gene neighborhood is highly conserved within the rhizobiales. Middle, *ptsP* locus. There is a predicted promoter sequence preceeding each gene, implying that they are not co-transcribed. Bottom, *ptsN* locus. All three genes are co-transcribed as a single operon. Arrows and gaps are drawn to scale.

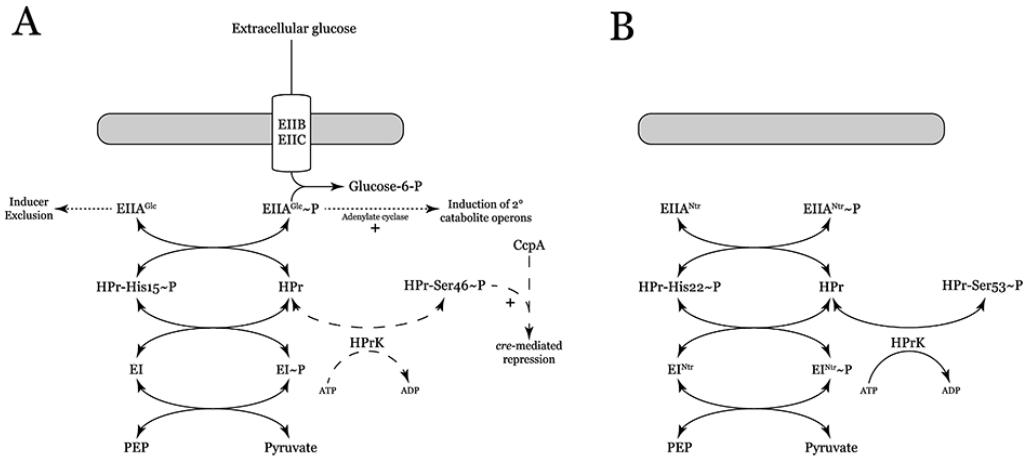

Figure 1.2 Model of canonical and *S. meliloti* PTS. A, combined model of *E. coli* and *B. subtilis* PTS. Dot arrows are pathways that only occur in *E. coli*, while dashed arrows only occur in *B. subtilis*. B, model of the *S. meliloti* incomplete PTS. Note the lack of associated sugar transporters and the presence of an HPrK in a Gram-negative organism.

Chapter 2
Materials and Methods

Strains, media, and plasmids. Strains and plasmids are listed in Table 1.1. *S. meliloti* was grown in tryptone-yeast extract (TY) or M9 minimal medium. *E. coli* was grown either in lysogeny broth (LB) or the auto-induction media described by Studier (115). Antibiotics were used at the following concentrations: streptomycin, 500 μg/mL; neomycin, 100 μg/mL; spectinomycin, 100μg/mL; ampicillin, 50 μg/mL; kanamycin, 25 μg/mL for cloning and 100 μg/mL for expression. Plasmids were delivered by electroporation in 1 mm gap-width cuvettes at 1.8 kV.

Construction of expression vectors. All expression vectors were based on pET-28a(+) (Novagen). All amplification steps were performed using Phusion DNA polymerase (NEB) and strain Rm1021 was used as the template. Primer sequences are listed in Table 2.2. The full-length *hpr* (*smc02754*) gene was amplified using primers hpr_UP and hpr_DOWN, and *ptsP* (*smc02437*) genes were amplified using primers ptsP_UP and ptsP_DOWN. The primers were designed to add an NheI site to the 5' end of each gene and an XhoI site or EcoRI site to *hpr* and *ptsP*, respectively. The GAF domain was amplified with primers ptsP_UP and GAF_DOWN, which encode NheI and BamHI sites, respectively. The PCR products were A-tailed, then cloned into pGEM T-Easy (Promega). Fragments were excised using the restriction enzymes listed above, then cloned into pET-28a(+) that had been digested with the corresponding restriction enzymes. The resulting plasmids pDG142H, pDG142P, and pRG07 (expressing his_6-tagged HPr, EI^{Ntr}, and EI_{GAF}, respectively) were sequenced to verify that no errors had been introduced during PCR or cloning steps.

Site-directed mutagenesis Site-directed mutants were generated using splicing overlap extension PCR (116). To clone *hpr*(R19L), the 5' end of the gene was amplified using primers hpr_UP and R19L_DOWN, and the 3' end of the gene was amplified using R19L_UP and hpr_DOWN. R19L_DOWN and R19L_UP each introduce the desired mutation and contain a sequence that is complimentary to the other primer. The two DNA fragments were then mixed and stitched together by PCR using primers hpr_UP and hpr_DOWN. The fragment was A-tailed, and cloned using the same method as pDG142H, resulting in plasmid pRG17. The *ptsP*(F102S) construct was built as above, except the primers used were ptsP_UP and F102S_DOWN for the 5' end of the gene and F102S_UP and ptsP_DOWN for the 3' end of the gene. The two fragments were stitched together using primers ptsP_UP and ptsP_DOWN, and then cloned as above, resulting in plasmid pRG09.

Expression of recombinant PTS proteins. Expression strains were inoculated into MDG medium and grown overnight at 37°C. For EI^{Ntr} constructs, the cells were then diluted 200-fold into ZYM-5052 and grown for 8 hours at 37°C. HPr constructs were diluted 500-fold into ZYM-522 and grown for 3 hours at 37°C. The temperature was decreased to 20°C and the culture was incubated an additional 20 hours. Cells were harvested by centrifugation at 4°C and pellets were stored at -20°C until purification.

Purification of EI^{Ntr}, and EI(F102S). Cell pellets were resuspended in buffer T (0.5 M NaCl, 25 mM imidazole, 25 mM TrisCl pH 7.4). The buffer was amended with halt protease inhibitors (Pierce), 1 mM dithiothreitol (DTT), 0.25 mg mL^{-1} lysozyme, and 2.5 U mL^{-1} benzonase (EMD Milipore). Cell suspensions were incubated for 2 hours on ice

and were sonicated for 6 minutes in 30-second bursts. The crude extract was clarified by centrifugation at 6,000 xg for 15 minutes, then 30,000 xg for 30 minutes. The lysate was passed through a 0.45 μm SFCA syringe filter (Corning) and loaded onto a 1 mL HisTrap FF Ni^{2+} column (GE Healthcare). The column was washed with 20 mL of buffer T and EI^{Ntr} was eluted with buffer T containing 0.5 M imidazole. The eluate was immediately diluted 2-fold in buffer containing 100 mM NaCl, 1 mM DTT, 5 mM magnesium acetate [$Mg(OAc)_2$], 20 mM TrisCl pH 7.4, 10% glycerol. 20 U of bovine thrombin (GE Healthcare) was added to the protein, which was dialyzed overnight at 4°C against 1 L of the dilution buffer, transferred to 0.5 L of fresh buffer and dialyzed an additional 5 hours. Protein retaining the his-tag was removed by passage back over the HisTrap FF column after equilibration in dialysis buffer. Untagged EI^{Ntr} was diluted 2-fold in 1 mM DTT, 25 mM TrisCl pH 8.0, and was applied to a 5 mL Q sepharose FF (GE Healthcare) column that had been equilibrated in buffer Q (50 mM NaCl, 1 mM DTT, 10 mM TrisCl pH 8.0). The column was washed with 50 mL of buffer Q and EI^{Ntr} was eluted with 5 mL steps of 75 mM, 100 mM, 125 mM, 150 mM, 250 mM, and 500 mM NaCl. Purified EI^{Ntr} was dialyzed at 4°C against 50 mM NaOAc, 1 mM DTT, 2 mM $Mg(OAc)_2$, 20 mM HEPES pH 8.0, 10% glycerol. The protein was passed through a 0.22 μm syringe filter and stored at -80°C.

Purification of HPr, HPr(R19L), and EI_{GAF}. For HPr, cell pellets were resuspended in buffer P (0.5 M NaCl, 25 mM imidazole, 20 mM $NaHPO_4$ pH 7.4) and the suspension was supplemented with halt protease inhibitors, 0.25 mg mL^{-1} lysozyme, and 2.5 U mL^{-1} benzonase. Cells were lysed and IMAC was performed as above, except in buffer P. The eluate was dialyzed at 4°C against 0.25 mL NaCl, 5 mM Na_2SO_4, 20 mM $NaHPO_4$ pH

7.4 10% glycerol. When HPr was used for native-PAGE assays the his-tag was removed as above. The protein was concentrated to 1mL using an amicon 3 kDa MWCO centrifugal filter (Millipore). The protein was applied to a 65 mL Superdex 75 (GE Healthcare) column equilibrated in buffer H (150 mM NaOAc, 5 mM Na_2SO_4, 20 mM HEPES pH 7.4, 10% glycerol). Eluted protein was concentrated as above, clarified with a 0.22 μm syringe filter and stored at -80°C. EI_{GAF} was purified using the same protocol, except glycerol was omitted from the dialysis buffer and Na_2SO_4 was omitted from all buffers.

Native PAGE assays. Reactions were assembled in 20 μL containing 0.1 M TrisOAc pH 8.0, 10 mM $Mg(OAc)_2$, 3 μg of untagged HPr and the indicated amount of EI^{Ntr}. Samples were pre-incubated at room temperature, and then the reaction was initiated by the addition of 10 mM PEP. The reactions were incubated for 15 minutes and room temperature and halted with the addition of ice-cold sample buffer (180 mM Tris, 120 mM CAPS, 20 mM EDTA, 12% sucrose final concentrations). Half of the reaction was loaded onto a 7.5% acrylamide gel buffered with 180 mM Tris, 120 mM CAPS (pH 9.6) (117). Gels were run at 75 V for 65 minutes and Coomassie stained.

Kinetics of HPr phosphorylation. EI^{Ntr} activity was measured using the lactate dehydrogenase (LDH) coupled assay (118) using a Synergy HT plate reader (BioTek) at 30°C. EI^{Ntr} was diluted to 1.6 μM in assay buffer (0.1 M NaOAc, 10 mM $Mg(OAc)_2$, 1 mM DTT, 0.1 M Na-HEPES pH 8.0) and incubated at 30°C for 15-60 minutes. Reactions were assembled in 200 μL of assay buffer with 10 U LDH (MP Bio), 150 μM NADH, 10 mM PEP, and the indicated amount of HPr. The reactions were initiated with the addition

of 40 nM EI^{Ntr} and the rate of HPr phosphorylation was measured using the absorbance at 340 nm. The data were corrected for oxidation of NADH by subtracting the ΔA_{340} of reactions lacking EI^{Ntr}. Data were measured in triplicate and fit with the Michaelis-Menten equation using Kaleidagraph 3.1 (Synergy software).

HPr phosphohydrolysis. Spontaneous dephosphorylation of HPr was measured using a modification of the LDH assay (119). Reactions contained 10 U LDH, 150 μM NADH, 1 μM EI^{Ntr} and the indicated amount of HPr in assay buffer (pH 7.5). The reactions were incubated for 15 minutes at 30°C and PEP was added to 10 mM. Under these conditions HPr will be completely phosphorylated within 10 seconds and the subsequent oxidation of NADH is due to HPr dephosphorylation.

Isothermal titration calorimetry (ITC). EI_{GAF} was dialyzed against 150 mM NaOAc, 100 mM HEPES pH 7.5, 1% glycerol at 4°C. The protein was passed through a 0.22 μm syringe filter and the final concentration was measured. The ligand was dissolved in dialysis buffer and filtered. Experiments were performed in a 1.8 mL cell volume VP-ITC apparatus (MicroCal) at 25°C with stirring at 300 rpm. A 2 μL test injection of the ligand was performed, followed by 28 injections of 10 μL each. The data were analyzed using the Origin software package (MicroCal) after discarding the data from the test injection.

Growth measurements. Starter cultures were grown in 3 mL M9 0.4% glycerol, then harvested by centrifugation and washed three times in carbon-free M9. Cells were inoculated at an OD_{595} of 0.005 into 200 μL of M9 with the indicated carbon source in 48 well plates (Falcon). The plates were incubated at 30°C with shaking every 10 minutes in

a Synergy HT plate reader (BioTek) and growth was measured by the OD_{595}. For *melA* expression experiments GFP fluorescence was measured with 480 nm excitation and 520 nm emission wavelengths.

Table 2.1 Strains and plasmids used in this study

Strain or plasmid	Description	Marker[a]	Reference
Strains			
Rm1021	*S. meliloti* wild-type, derived from SU-47	Sm	120
CAP95	Rm1021 Δ*hpr*, *rhaS*::*hpr*S53A	SmNm	111
CAP49	Rm1021 Δ*hpr*, *rhaS*::*hpr*	SmNm	111
BL21(DE3)	T7 Expression strain		
XL1Blue MRF'	Cloning strain	Tc	
Plasmids			
pCAP11	pMB393 P*melA*::*gfp*	Sp	110
pDG142H	pET-28a with wild-type *hpr*	Km	121
pDG142P	pET-28a with wild-type *ptsP*	Km	121
pRG07	pET-28a with *ptsP* GAF domain	Km	121
pRG09	pET-28a with *ptsP* F102S	Km	This study
pRG17	pET-28a with *hpr* R19L	Km	This study
pRG47	pET-28a with *ptsP* F102S GAF domain	Km	This study
pET-28a(+)	His-tag expression vector; T7 promoter	Km	Novagen
pGEM T-easy	Cloning vector	Ap	Promega

[a] Resistance markers: Sm, streptomycin; Nm, neomycin; Km, kanamycin; Ap, ampicillin; Tc, tetracycline; Sp, spectinomycin

Table 2.2 Primers used in this study

Primer	Sequence (5'-3')[a]	Description
hpr_UP	ATGATGGCTAGCCGCCCCGACACGGCTCT	5' end of *hpr* with NheI site
hpr_DOWN	ATGTTTACTCGAGTCACATCTCTTCG	3' end of *hpr* with XhoI site
ptsP_UP	CACGCGATGGCTAGCCTTTCCGCAGGTCCGCG	5' end of *ptsP* with NheI site
ptsP_DOWN	CTCTTGGAATTCCTAAACCGGTATGCCGT	3' end of *ptsP* with EcoRI site
GAF_DOWN	GGATCCTCAGGTCGCGACCATCTCGG	3' end of the GAF domain, BamHI site
R19L_DOWN	ATGCAGGCCCAGTTTGTTGACGAT	Internal primer for construction of *hpr*(R19L)
R19L_UP	ATCGTCAACAAACTGGGCCTGCAT	Internal primer for construction of *hpr*(R19L)
F102S_DOWN	CAGGTAGGTCGAGGCGGGGTG	Internal primer for construction of *ptsP*(F102S)
F102S_UP	CACCCCGCCTCGACCTACC	Internal primer for construction of *ptsP*(F102S)

[a]Underlined portion of the sequence corresponds to the engineered restriction site

Chapter 3
Characterization of EI^{Ntr} *

Characteristics of the carbohydrate-type Enzyme I. The carbohydrate Enzyme I is comprised of two domains that can be separated by protease digestion. The N-terminal domain, which is homologous to the swivel domain of pyruvate phosphate dikinase (PPDK), contains the phosphorylated histidine, and is responsible for HPr binding. The C-terminal domain binds PEP and mediates dimerization (122). Dimerization of EI is required for activity (though each subunit can be phosphorylated simultaneously), and occurs at a very low rate. The EI dimer in enteric bacteria is cold sensitive, and will dissociate at reduced temperatures (123). Autophosphorylation (and to a large extent dimerization) of EI requires both the phospho-donor PEP, as well as a divalent cation (preferably Mg^{2+}) (89). EI phosphorylation of HPr is a Ping Pong Bi Bi reaction, with a k_{cat}/K_M that typically approaches the diffusion limit (124-126).

In *E. coli*, the carbohydrate EI is inhibited by the TCA cycle intermediate α-ketoglutarate (127). In bacteria α-ketoglutarate, consumed during assimilation of ammonium, is used as a measure of carbon levels for balancing carbon and nitrogen metabolism (128). This inhibition may serve as a method of reducing carbon uptake during nitrogen-limiting growth, which would prevent carbon overflow in the TCA cycle. Coupling EI activity to α-ketoglutarate levels allows the cell to maintain the balance of carbon and nitrogen acquisition during growth. It has since been proposed that cAMP

* Portions of this chapter have been previously published. Reference: Goodwin RA, Gage DJ. 2014. Biochemical characterization of a nitrogen-type phosphotransferase system reveals that Enzyme I^{Ntr} integrates carbon and nitrogen signaling in *Sinorhizobium meliloti*. J Bacteriol 196:1901-1907

signaling, which is controlled by the PTS (and therefore EI), partitions the proteome between catabolic and biosynthetic genes (129).

The nitrogen-type Enzyme I. The PTS^{Ntr} contains an EI paralog, encoded by the gene *ptsP*, that contains an N-terminal GAF domain (130). In *E. coli*, EI^{Ntr} is activated by α-ketoglutarate and inhibited by glutamine, both of which are likely detected via its GAF domain (131). Initial characterization of EI^{Ntr} activity revealed a 1000-fold decrease in its activity relative to EI, although there are troubling aspects to this work that will be discussed below (132). In preparation for structural studies Piszczek et al. found that perdeuteration of a truncated EI^{Ntr} lacking a GAF domain exhibited decreased stability (133). In *Bradyrhizobium japonicum*, mutants containing Tn5 insertions in *ptsP* or *lysC* (the gene immediately upstream of *ptsP* in many α-proteobacteria) abolished oligopeptide uptake (134). Purified EI^{Ntr} from *B. japonicum* can only autophosphorylate using PEP, but not ATP, as a substrate. However, co-incubation of *B. japonicum* EI^{Ntr} with crude cell extracts results in ATP-dependent phosphorylation of the protein, implying that it can be phosphorylated by another enzyme within the cell. Pull-down assays showed that EI^{Ntr} interacts directly with the enzyme aspartokinase (the product of the *lysC* gene), and that purified aspartokinase inhibits ATP-dependent phosphorylation of EI^{Ntr} by cell extracts.

The GAF domain. GAF (cGMP-specific and -stimulated phosphodiesterases, *Anabaena* adenylate cyclases, and *E. coli* FhlA) domains are small molecule sensing domains that are found throughout the three kingdoms of life (135). While it was recognized that proteins such as NifA had discreet sensory domains, the GAF domain was only recognized as a unified group during analysis of PAS domain containing phytochromes

and adenylate cyclases. GAF domains are frequently found in signal transducing proteins, including phosphodiesterases, transcriptional regulators, as well as the phosphotransferase EI^{Ntr}. In *Azotobacter vinelandii* there is a GAF domain containing protein that is responsible for regulating each of the three nitrogenases. NifA regulates the molybdenum-iron containing nitrogenase-1, VnfA controls the vanadium-iron containing nitrogenase-2, and AnfA controls the iron-only nitrogenase-3. The GAF domains of VnfA and AnfA bind iron-sulfur clusters, which are used to sense the redox state of the cell (136). In contrast, the GAF domain of NifA (which shares considerable sequence homology with EI^{Ntr}) binds α-ketoglutarate directly, and senses the redox state of the cell through interaction with the protein NifL (137).

Nitrogen stress response. In many proteobacteria the general nitrogen stress response (NSR) is mediated by the *ntr* and *gln* systems, both of which have been characterized in *S. meliloti* (138). The *ntr* genes regulate a number of processes during nitrogen-limited growth, but deletions in these genes do not impact symbiosis (139, 140). Mutations within the regulatory *gln* genes cause defects in nitrogen acquisition during free-living growth and complex phenotypes during symbiosis (141, 142). *S. meliloti* has three glutamine synthetases (GS), encoded by the genes *glnA* (GSI), *glnII* (GSII), and *glnT* (GSIII) (143). *glnT* is a cryptic gene, and its expression has only been detected when *glnA* and *glnII* are deleted. At the center of the glutamine regulatory cascade is the bifunctional uridylyltransferase/cleavage enzyme GlnD (144). In enteric bacteria, and likely *S. meliloti*, GlnD detects the intracellular ratio of [α-ketoglutarate]:[glutamine], which is a proxy for overall nitrogen status (128). Nitrogen scarcity stimulates uridylylation of the P_{II} proteins GlnB and GlnK by GlnD, while nitrogen excess triggers

removal of the uridylyl groups by GlnD (144). Uridylylated P_{II} proteins interact with GlnE, which then adenylylates GSI. Adenylylation of GSI inactivates it, preventing assimilation of NH_4^+ through synthesis of glutamine. Uridylylated GlnB (but not GlnK) stimulates the activity of the histidine kinase NtrB (145). NtrB phosphorylates the response regulator NtrC, which in turn activates transcription of genes such as *amtB*, *glnII*, and *glnA*. In *E. coli*, unmodified GlnK binds AmtB, blocking uptake of ammonium in nitrogen-replete conditions (146).

While *glnD* appears to be an essential gene, *Tn5* insertions have been isolated in the 5' end of the gene, and truncation mutants have been isolated that express GlnD without the first 70 aa of the protein (141). The *glnD* truncation mutant is able to infect *M. sativa*, forming healthy pink nodules that fix nitrogen at nearly the same rate as nodules formed by wild-type strain Rm1021. However, the dry-mass of plants infected with the *glnD* mutant are only half of those infected with wild-type strain Rm1021. When nitrogen accumulation is traced using $^{15}N_2$, the fixed nitrogen initially accumulates within plant tissue, but is lost from the plant (through an unknown process) within 24 hours. Mutations in both the *ntr* and *gln* genes results in growth defects on nitrogen sources such as potassium nitrate (*ntrC*) or amino acids (*gln*) (139, 142). Yurgel et al. suggested that GlnD interacts with additional partners independent of its uridylylation of the P_{II} proteins (142). This hypothesis is based on the fact that phenotypes observed in the *glnD* partial deletion are absent in *glnBglnK* strains as well as a strain expressing GlnB(Y51F), which can not be uridylylated by GlnD.

S. meliloti EI^{Ntr}. In *S. meliloti*, the only Enzyme I homolog is a nitrogen-type EI with an N-terminal GAF domain. Early attempts at deleting *ptsP* (the gene that encodes EI^{Ntr})

were unsuccessful, leading us to believe that it is an essential gene. While the gene has been deleted since then, the resulting mutant displays a severe growth defect that prevents physiological characterization of the Δ*ptsP* mutant. As an alternative we have taken a biochemical approach to characterization of EI^{Ntr}. The work described in this chapter centers around regulation of EI^{Ntr}, specifically how the protein responds to signals emanating from central metabolism. From these studies a model was built describing how SMCR is regulated through changes in EI^{Ntr} activity. Previous work combining genetic and physiological experiments suggest that SMCR is strengthened when the flow of phosphate through HPr-His increases. The histidine of HPr is likely only phosphorylated by EI^{Ntr}, which implies that imposition of SMCR will be strongly coupled to the activity of this enzyme.

Results

Expression and purification of SmPTS proteins. In order to characterize EI^{Ntr} and HPr both proteins were expressed with N-terminal his-tags. Expression of both EI^{Ntr} and HPr at 37°C using IPTG resulted in completely insoluble protein and an alternative method needed to be developed. Auto-induction, which was developed by Studier, is a technique that uses medium components (specifically glucose and lactose) to regulate expression of genes regulated by the Lac repressor (115). Optimization of auto-induction protocols allowed for soluble expression of both EI^{Ntr} and HPr. Initial purification of both proteins was performed using Ni immobilized metal affinity chromatography (IMAC). Following IMAC EI^{Ntr} was further purified using anion exchange chromatography, while HPr was purified using size exclusion chromatography. These protocols resulted in approximately

5 mg and 15 mg of purified HPr and EI^{Ntr} per liter of culture medium, respectively (Fig. 3.1).

Phosphorylation of HPr by EI^{Ntr}. Phosphorylation of HPr can be observed using the change in electrophoretic mobility of P~HPr due to the increased negative charge, and this method was used to show that *S. meliloti* EI^{Ntr} is capable of phosphorylating its cognate HPr. EI^{Ntr} and HPr were incubated together and the reactions were separated on a 7.5% native polyacrylamide gel buffered with Tris/CAPS (117). The gel was stained with Coomassie blue and showed that EI^{Ntr} phosphorylated HPr in a PEP-dependent manner (Fig. 3.3). While carbohydrate type Enzymes I phosphorylate HPr at very high rates there are little data on the activity of EI^{Ntr}. The *E. coli* EI^{Ntr} was previously characterized, and shown to have a turnover number 1000-fold lower than that of EI (132). However, there are two problems with this study: the EI^{Ntr} was purified and refolded from inclusion bodies, and the enzyme was assayed using a non-native mannitol phosphorylation assay. The use of refolded protein is especially concerning, since the preparations were insensitive to glutamine, which was recently shown to be an inhibitor of the *E. coli* EI^{Ntr} (131). Here, I measured the activity of EI^{Ntr} using the lactate dehydrogenase (LDH) coupled assay (118). EI^{Ntr} phosphorylation of HPr was measured with HPr concentrations ranging from 2.5 μM to 50 μM. The data were fit to the Michaelis-Menten equation, from which the K_m and k_{cat} were calculated (Fig. 3.2). The K_m of EI^{Ntr} for HPr was found to be 12.8 ± 1.5 μM, the k_{cat} 1.11±0.4 s^{-1}, resulting in a k_{cat}/K_m of 8.67×10^4 $M^{-1}s^{-1}$.

EI^{Ntr} is inhibited by glutamine. CAP95 (Δ*hpr*, *rhaS*::*hpr*S53A) is a strain that shows an increase in SMCR relative to wild type strain Rm1021, likely due to over-phosphorylation of HPr by EI^{Ntr}. Previously, a transposon mutagenesis screen had been

performed in CAP95 to find mutants with reduced SMCR (measured by the formation of blue colonies on M9 agar containing succinate, lactose, and X-gal). Among the mutants with increased β-galactosidase activity were *glnD* and *glnE*, both involved in glutamine regulation in *S. meliloti* (unpublished results). From these data we predicted that glutamine (or another metabolite involved in ammonium assimilation) might have an influence on PTS activity. When EI^{Ntr} reactions were set up with increasing amounts of glutamine and analyzed by native-PAGE there was a marked decrease in the amount of P~HPr (Fig. 3.3). Glutamine inhibition of EI^{Ntr} was further analyzed using the continuous LDH assay. These assays confirmed that the EI^{Ntr} activity decreased in the presence of glutamine. Addition of 1 mM glutamine, a physiologically relevant concentration, to assays containing 20 μM HPr reduced EI^{Ntr} activity by 80% (Fig. 3.4).

The GAF domain of EI^{Ntr} binds glutamine. GAF domains are often responsible for detecting cellular status by sensing small molecule effectors (135, 137, 147). We reasoned that the GAF domain found in EI^{Ntr} might be responsible for glutamine binding. In order to test this a fragment of the *ptsP* gene encoding the GAF domain (residues 1-164) was cloned into pET-28a(+) for expression as a his-tagged construct and purification. Binding of glutamine by the isolated GAF domain was measured using ITC. Titration of glutamine into the GAF domain resulted in an exothermic binding curve. From the binding curve it was determined that the GAF domain binds glutamine at a 1:1 molar ratio with a K_D of 35 μM (Fig. 3.5).

EI^{Ntr} residue F102 is required for glutamine binding. When a site-directed mutant was made in the *A. vinelandii* NifA, replacing F119 with a serine, the protein lost its ability to bind α-ketoglutarate. Alignment of the GAF domains from *A. vinelandii* NifA, *S. meliloti*

EI^{Ntr}, and *E. coli* EI^{Ntr} revealed that these small-molecule binding domains all contain a phenylalanine at the same position (Fig. 3.6). To determine if F102 was also required for glutamine inhibition of *S. meliloti* EI^{Ntr} a plasmid expressing an F102S site-directed mutant was constructed. The protein was expressed and purified in the same manner as the wild-type enzyme and its sensitivity to glutamine was assayed. The phosphorylation of 20 μM HPr was measured and compared to the rate of phosphorylation in the presence of 10 μM, 100 μM, and 1000 μM of glutamine. The EI^{Ntr}(F102S) mutant showed no inhibition in any of these glutamine concentrations, indicating that this residue is required for glutamine inhibition of *S. meliloti* EI^{Ntr} (Fig. 3.7).

The *S. meliloti* EI^{Ntr} is insensitive to α-ketoglutarate. EI^{Ntr} of *E. coli* is both inhibited by glutamine and activated by α-ketoglutarate (131). Since α-ketoglutarate is a substrate for LDH the gel-shift assay was used to determine its impact on EI^{Ntr} activity. HPr phosphorylation reactions were set up with amounts of EI^{Ntr} that would phosphorylate 50% of the HPr after 10 minutes. The reactions were supplemented with varying amounts of α-ketoglutarate and the extent of HPr phosphorylation was determined using native-PAGE (Fig. 3.8A). Addition of α-ketoglutarate did not cause an increase in the fraction of phosphorylated HPr, implying that α-ketoglutarate has no affect on the activity of EI^{Ntr}. To show that the insensitivity was not due to the preparation of EI^{Ntr} a control reaction was included that contained 10 mM glutamine. The HPr from this reaction was largely unphosphorylated, showing that EI^{Ntr} was still inhibited by glutamine. Another possibility was that α-ketoglutarate does not influence EI^{Ntr} activity directly, but could compete with glutamine for binding EI^{Ntr} and therefore attenuate inhibition. Reactions were assembled containing 5 mM glutamine and a range of α-ketoglutarate

concentrations and were analyzed using native-PAGE. Addition of α-ketoglutarate to each of the reactions did not relieve EI^{Ntr} inhibition (Fig 3.8B).

Glutamine decreases the strength of SMCR. In our model of the *S. meliloti* PTS, phosphorylation of HPr-His strengthens SMCR (111). Since EI^{Ntr} is inhibited by glutamine *in vitro*, we reasoned that increasing glutamine *in vivo* would result in a relief of catabolite repression. *S. meliloti* strain Rm1021 was grown in M9 minimal medium containing 0.05% succinate, 0.1% raffinose, and a range of glutamine concentrations. Growth measurements showed that in the presence of glutamine the diauxic lag exhibited by strain Rm1021 decreases significantly, resembling the phenotype of the Δ*hpr* strain. These experiments were repeated with the P*melA*::*gfp* reporter strain and the culture fluorescence was followed throughout the growth curve. When glutamine was added to the medium *melA* promoter activity increased sooner and reached a higher level than when the strain was grown in the absence of glutamine (Fig 3.9). Strain CAP95 (Rm1021 Δ*hpr*, *rhaS*::*hpr*S53A) has an enhanced SMCR phenotype, likely due to overphosphorylation of HPr-His. Serial dilutions of CAP95 were spotted onto SLX plates (M9 agar containing 0.05% succinate, 0.1% lactose, and X-gal) either with or without 0.2% glutamine. When the plates lacking glutamine were incubated, CAP95 formed smaller, whiter colonies relative to the control strain CAP49 (Rm1021 Δ*hpr*, *rhaS*::*hpr*). Colonies from strain CAP95 grown with glutamine were larger in size and a darker blue, although the phenotype did not completely revert to that of strain CAP49 (Fig 3.10).

Discussion

While carbohydrate Enzymes I have been extensively characterized over the past 50 years there is little information on EI from incomplete PTS. The N-terminal GAF domain appears to be responsible for the propensity of purified EI^{Ntr} to aggregate, necessitating the addition of solubility tags or refolding protein purified from inclusion bodies (133). The enzyme has been primarily studied in *E. coli*, while no work has been done in other bacteria beyond its ability to phosphorylate HPr (112, 148, 149). It was shown that purified EI^{Ntr} from *E. coli* is inhibited by glutamine and activated by α-ketoglutarate (131).

I have reported here a method for purification of both EI^{Ntr} and HPr in quantities sufficient for biochemical characterization. The turnover number of EI^{Ntr} is dramatically lower than that of the carbohydrate-type homologs. The lower activity may reflect the incomplete nature of the *S. meliloti* PTS. In a carbohydrate PTS the rate of sugar import (and therefore growth rate) depends on the rate of PTS activity (150). Because incomplete phosphotransferase systems presumably play a regulatory role independent from sugar uptake their activity is likely uncoupled from the growth rate of an organism and does not require significant phosphate flux through the system. Furthermore, a high rate of phosphorylation would cause rapid saturation of incomplete PTS due to the lack of a phosphate sink, rendering it incapable of responding to changing nutrient availability.

When the PTS^{Ntr} was originally named there was little evidence for its involvement in nitrogen regulation beyond the *ptsN* gene being in the same operon as *rpoN* (95). Recently, biochemical evidence has shown that the *E. coli* EI^{Ntr} is regulated by both glutamine and α-ketoglutarate, which are metabolites frequently associated with

nitrogen regulation in Gram-negative bacteria. While studying the phosphorylation of HPr by *S. meliloti* EI^{Ntr} it was found that glutamine inhibited the reaction, while α-ketoglutarate had no effect on it. Glutamine inhibited EI^{Ntr} primarily at micromolar to millimolar concentrations, which is the same range that has been found for intracellular glutamine pools in *E. coli* (151). Direct binding measurements between the GAF domain of EI^{Ntr} and glutamine showed that the K_D was 35 μM. Interestingly, these data indicate that even during nitrogen limited growth EI^{Ntr} within the cell should be largely inhibited. According to our model, inhibition of *S. meliloti* EI^{Ntr} by glutamine should result in weakened SMCR. Indeed, addition of glutamine caused a large decrease in the length of diauxic lag in strain Rm1021. While this supports our model we cannot rule out the possibility that glutamine affected the physiology of *S. meliloti* at a more general level than reducing PTS activity (i.e. if an increase in the intracellular amino acid pool supported a higher rate of MelA and AgpABCD synthesis it could decrease the amount of time required to exit diauxic lag).

Alignment of the GAF domains from *A. vinelandii* NifA and EI^{Ntr} from both *E. coli* and *S. meliloti* showed that all three contained a phenylalanine at the same position. Since this residue is required for NifA binding of α-ketoglutarate, a metabolite that is structurally similar to glutamine, it seemed likely that it may also be required for effector binding in *S. meliloti* EI^{Ntr}. Kinetic experiments showed that the EI^{Ntr}(F102S) mutant was uninhibited by the addition of glutamine. The kinetic data should be complemented by measuring the binding affinity of GAF(F102S) for glutamine. This construct has been built, and the protein purified, but it has yet to be studied. This finding could be advantageous for studying the *in vivo* effect of glutamine on SMCR. If the weakened

SMCR exhibited by cells grown in the presence of glutamine was due to inhibition of EI^{Ntr}, then a strain expressing only EI^{Ntr}(F102S) should be insensitive to addition of glutamine and show no reduction in the length of the diauxic lag. This approach is not without difficulties. We initially believed that *ptsP* was an essential gene due to an inability to isolate mutants with an in-frame deletion of the gene. When the suicide plasmid used for deletion of *ptsP* was redesigned, in-frame mutants were isolate, but they showed significant growth defects and accumulated suppressor mutations at such a high rate that they could not be used (data not shown). The other difficulty is that mutants with overphosphorylated HPr also show significant growth defects. Presumably, EI^{Ntr} will be partially inhibited during growth on NH_4Cl due to its glutamine pool. In a strain expressing EI^{Ntr}(F102S) HPr would likely be overphosphorylated regardless of the growth conditions.

Despite the direct connection between the *S. meliloti* PTS and SMCR, EI^{Ntr} is insensitive to α-ketoglutarate, a common signal of carbon availability within the cell. This stands in contrast to the α-ketoglutarate activated *E. coli* EI^{Ntr}, which is involved not in CCR, but general regulation of cellular homeostasis. The unusual CCR hierarchy in *S. meliloti* and the control of EIIA phosphorylation state provide an explanation for this difference. From a strictly equilibrium point of view the phosphorylation state of EIIA in the cell is determined by the ratio of [PEP]:[pyruvate] (152). When *E. coli* is grown on its preferred substrate glucose, this ratio is dependent on the carbon flux from glycolysis. On the other hand, α-ketoglutarate acts as a signal for the carbon pool within the TCA cycle, carbon available for biosynthetic pathways. In *S. meliloti*, succinate is the preferred carbon source and the [PEP]:[pyruvate] ratio is set not by glycolysis, but

gluconeogenesis. During gluconeogenesis the production of these two metabolites is controlled separately, where PEP is synthesized by PEP carboxykinase and the malic enzyme synthesizes pyruvate (55). In this case succinate and α-ketoglutarate represent the same general carbon pool, making a response to α-ketoglutarate pools by EI^{Ntr} redundant. If this model for carbon regulation in *S. meliloti* holds true, then it could explain why *pckA*, the gene encoding PEP carboxykinase, is found within the same chromosomal locus as *hprK*, *manX*, and *hpr* in a majority of the rhizobiales.

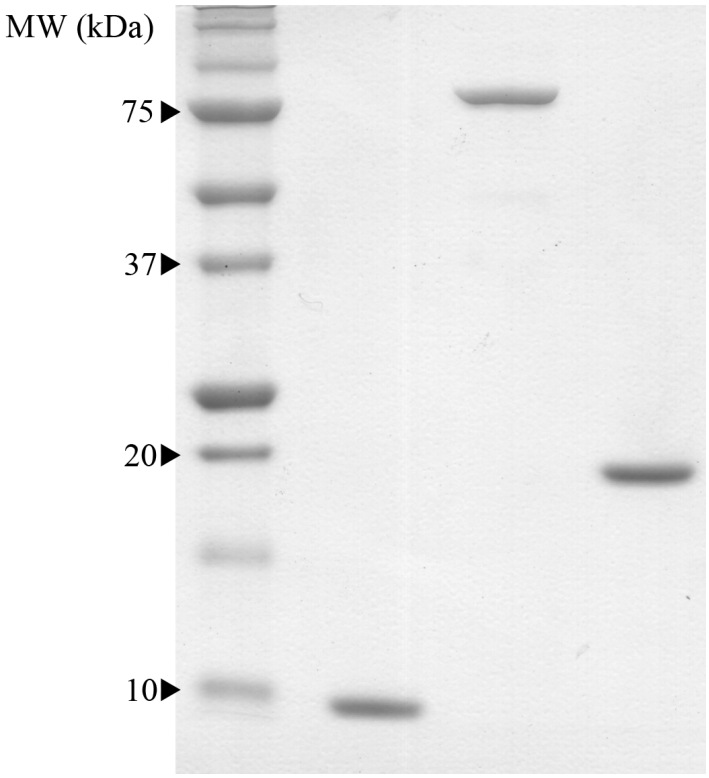

Figure 3.1 Purified PTS proteins separated on a 12% TrisOAc gel and stained with colloidal coomassie G-250. Lane 1, Bio-Rad Precision Plus protein standards; lane 2, purified HPr; lane 3, EI^{Ntr}; lane 4, EI_{GAF}. 1 μg of protein was loaded in each lane.

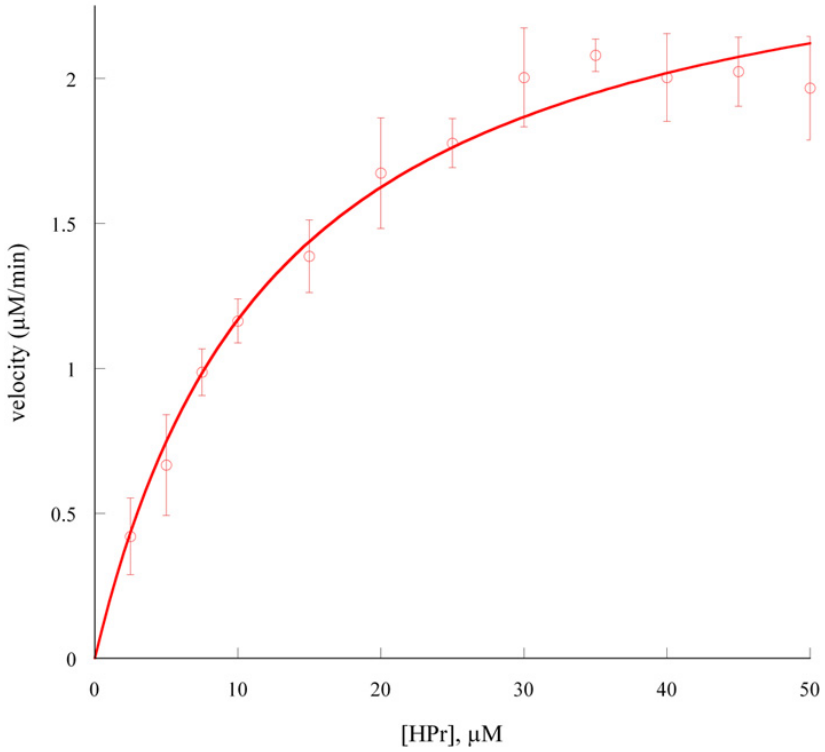

Figure 3.2 Kinetics of HPr phosphorylation by EI^{Ntr}. Phosphorylation rates were measured using the LDH-coupled assay with 40 nM EI^{Ntr} in 100 mM NaOAc, 10 mM PEP, 10 mM $Mg(OAc)_2$, 1 mM DTT, 100 mM Na-HEPES pH8.0. Reactions were performed for each of the indicated concentrations of HPr, in triplicate, and data points are the mean ± standard deviation. The line represents a fit to the Michaelis-Menten equation.

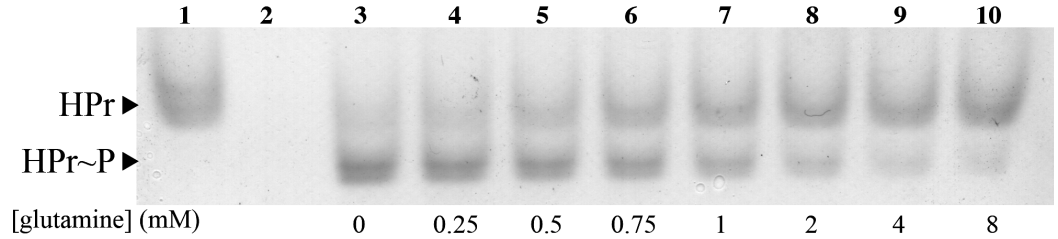

Figure 3.3 Inhibition of EI^{Ntr} activity by glutamine. Reactions contained 100 ng of EI^{Ntr}, 3 μg HPr, 10 mM $Mg(OAc)_2$, 1 mM DTT, 0.1 M Tris-OAc pH8.0, and the indicated concentrations of glutamine in 20 μL total volume. Reactions were incubated for 10 minutes, and then mixed with sample buffer and half of the reaction was loaded on a 7.5% polyacrylamide Tris/CAPS gel pH9.6. Lane 1, reaction lacking PEP; lane 2, reaction lacking HPr; lanes 3-10, reactions containing the indicated concentration of glutamine.

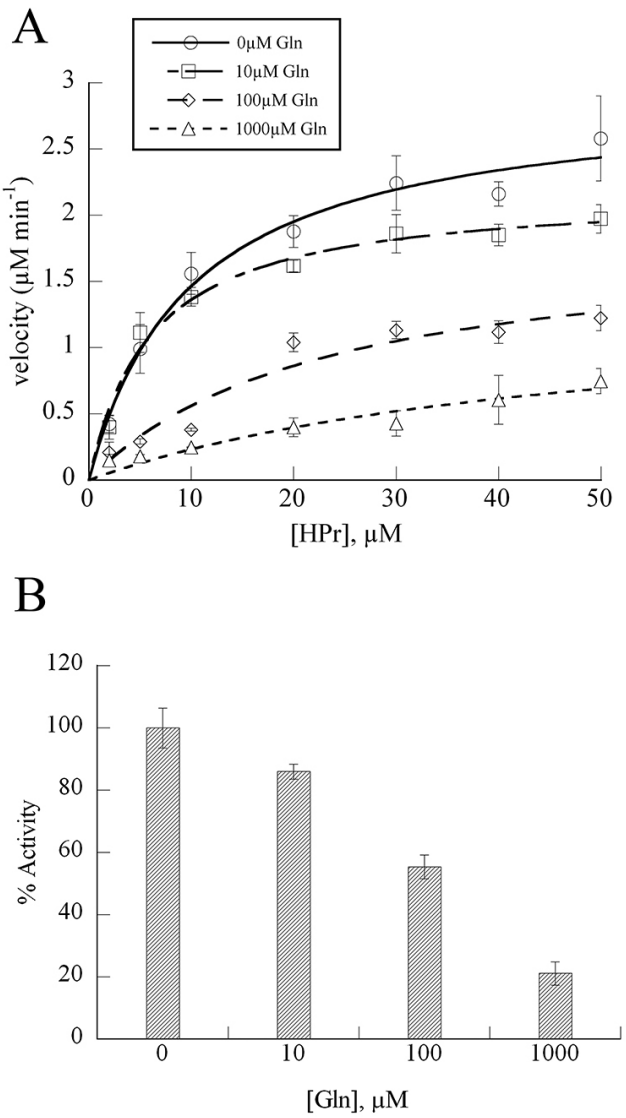

Figure 3.4 Kinetic measurements of EI^{Ntr} inhibition by glutamine. LDH assays were performed as in figure 3.2 with the addition of the indicated concentrations of glutamine. A, data points represent the mean of three measurements and bars represent the standard deviation. B, EI^{Ntr} phosphorylation of 20 μM HPr and the indicated concentration of glutamine represented as percent activity (relative to reactions performed in the absence of glutamine).

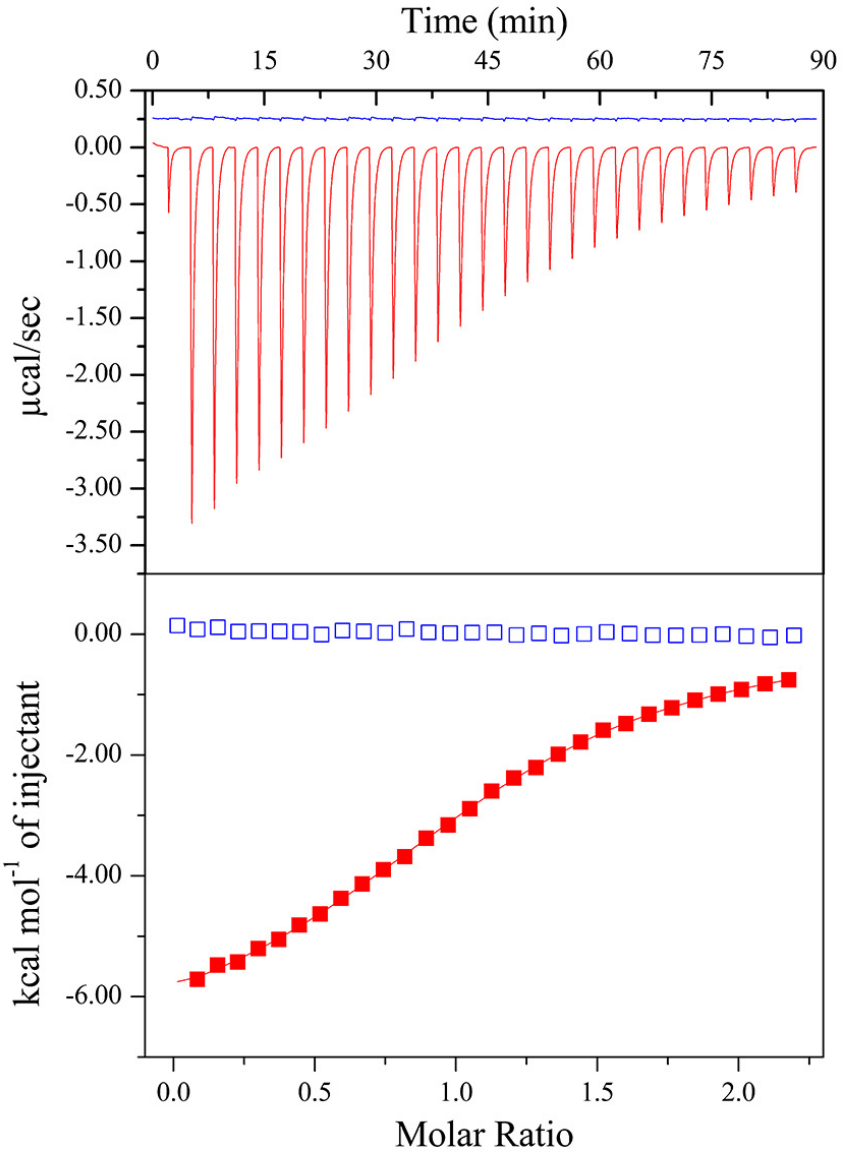

Figure 3.5 ITC measurements of EI_{GAF} binding to ligand. EI_{GAF} was dialyzed against 150 mM NaOAc, 50 mM Na-HEPES pH7.5, 1% glycerol, and then diluted to 143 µM. The cell contained 1.8 mL of protein maintained at 25°C. The syringe contained 1.5mM glutamine (red), or α-ketoglutarate (blue), dissolved in dialysis buffer. A 2 µL test injection of ligand was made followed by 28 injections of 10 µL each. Top, raw heat of titration (α-ketoglutarate data were shifted upwards by 0.25 µcal/sec for clarity); Bottom, binding isotherm calculated by integration of each injection peak. Data for glutamine were fit to a one-site binding model using Origin software (MicroCal).

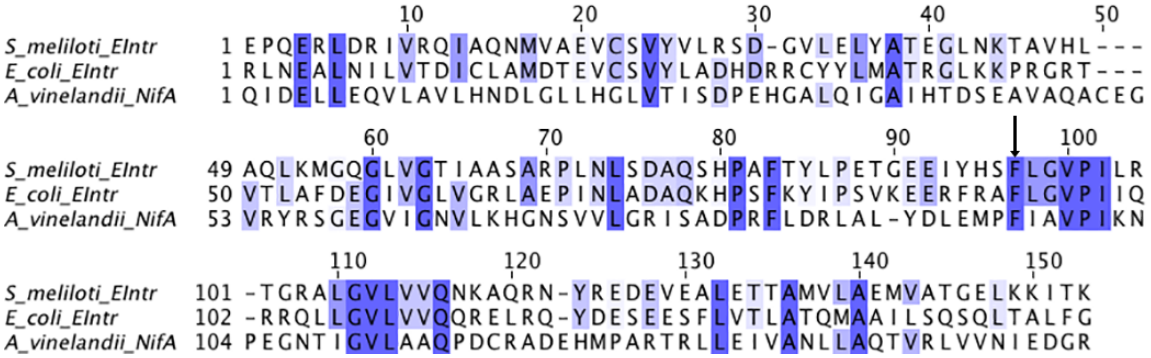

Figure 3.6 MUSCLE Alignment of GAF domains that bind small molecules. *S. meliloti* EI^{Ntr} and *E. coli* EI^{Ntr} bind glutamine; *E. coli* EI^{Ntr} and *A. vinelandii* NifA bind α-ketoglutarate. The arrow indicates a phenylalanine that is important in substrate binding in *A. vinelandii* NifA. Residues are shaded by percent identity, with dark blue representing 100% and white representing 0%. The limits of the GAF domain were determined using the SMART database (http://smart.embl-heidelberg.de).

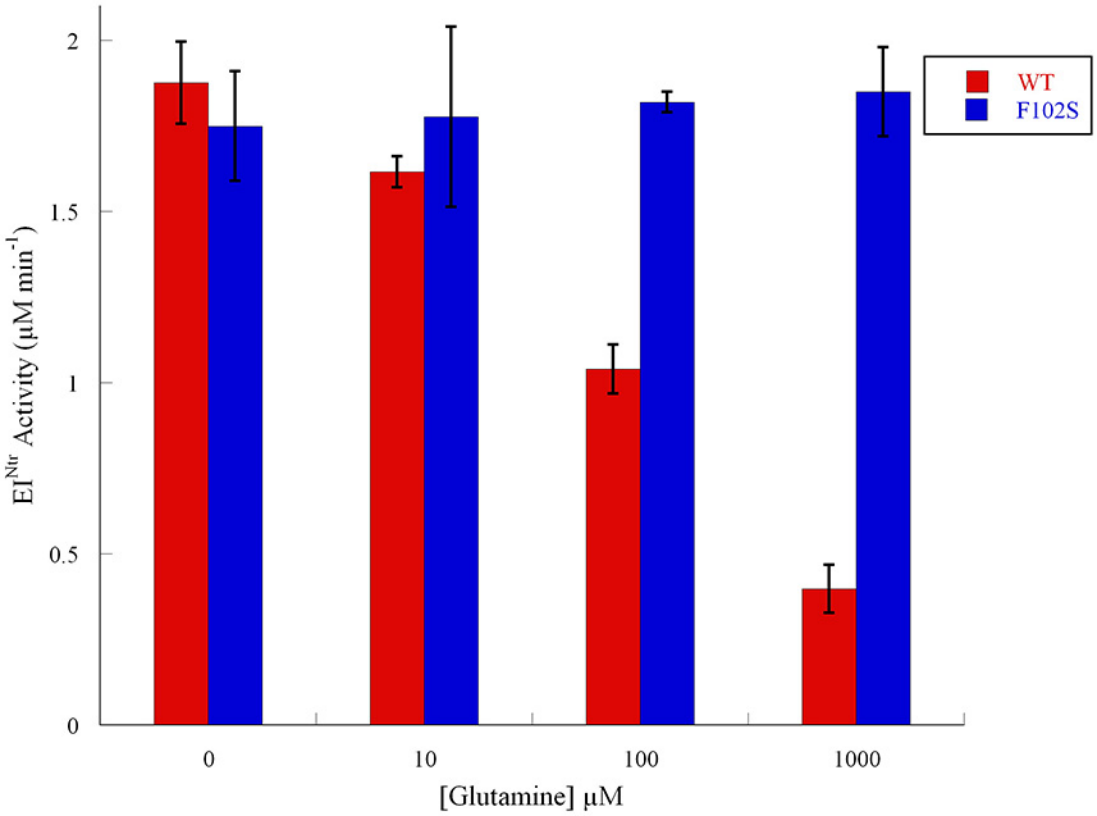

Figure 3.7 Inhibition of EI^{Ntr} and EI^{Ntr}(F102S) by glutamine. Enzyme activity was measured with the LDH assay using 20 μM HPr and the indicated concentration of glutamine. Blue, wild-type EI^{Ntr}; Red, EI^{Ntr}(F102S). Values represent the mean of three replicates and error bars represent the standard deviation.

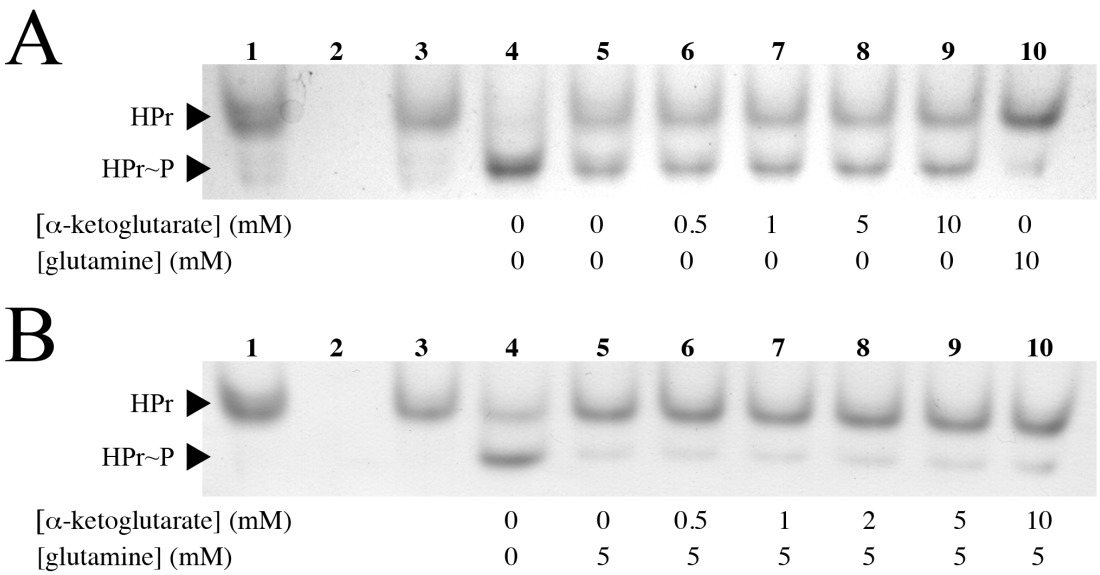

Figure 3.8 Effect of α-ketoglutarate on EI^{Ntr}. Phosphorylation reactions were performed as above, with the following modifications. For both gels: lane 1, reaction lacking EI^{Ntr}; lane 2, reaction lacking HPr; lane 3, reaction lacking PEP. A, HPr was phosphorylated by 50 ng of EI^{Ntr} in the presence of the indicated concentrations of α-ketoglutarate or glutamine. B, HPr was phosphorylated by 100 ng of EI^{Ntr} in the presence of 5mM glutamine and the indicated concentrations of α-ketoglutarate.

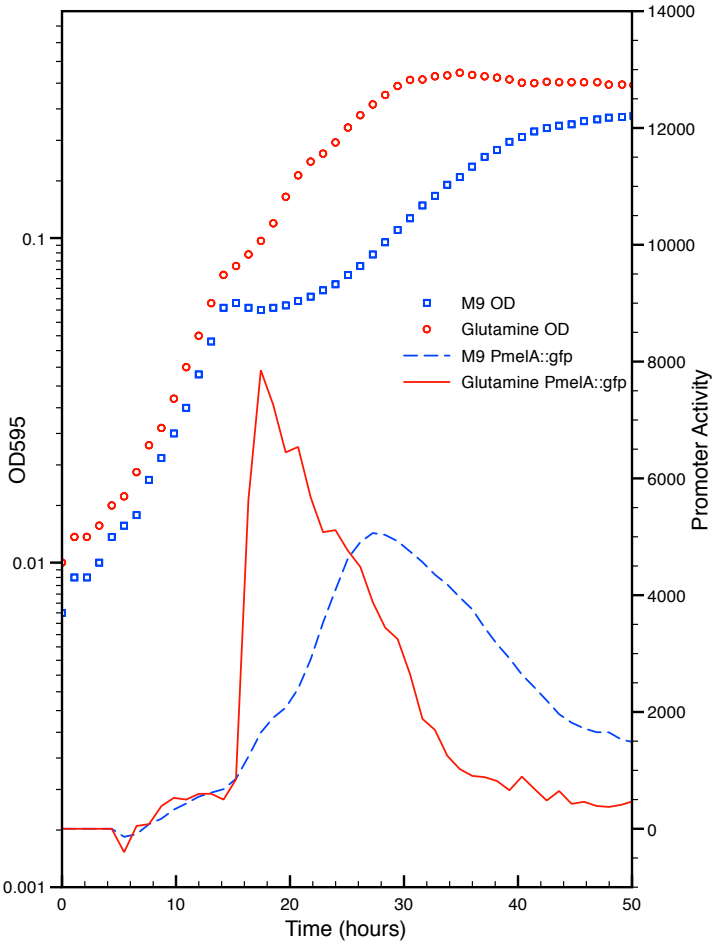

Figure 3.9 Diauxic growth of strain Rm1021 in the presence or absence of glutamine. Strain Rm1021 harboring pCAP11, which carries a P_{melA}::*gfp* transcriptional fusion, was grown in M9 containing 0.05% succinate and 0.1% raffinose with (red) or without (blue) 0.1% glutamine. Individual points are the OD_{595} of the culture. Lines represent the promoter activity, which is calculated as the [Δfluorescence/Δt]/OD_{595} calculated from 5 fluorescence readings surrounding each OD_{595} measurement.

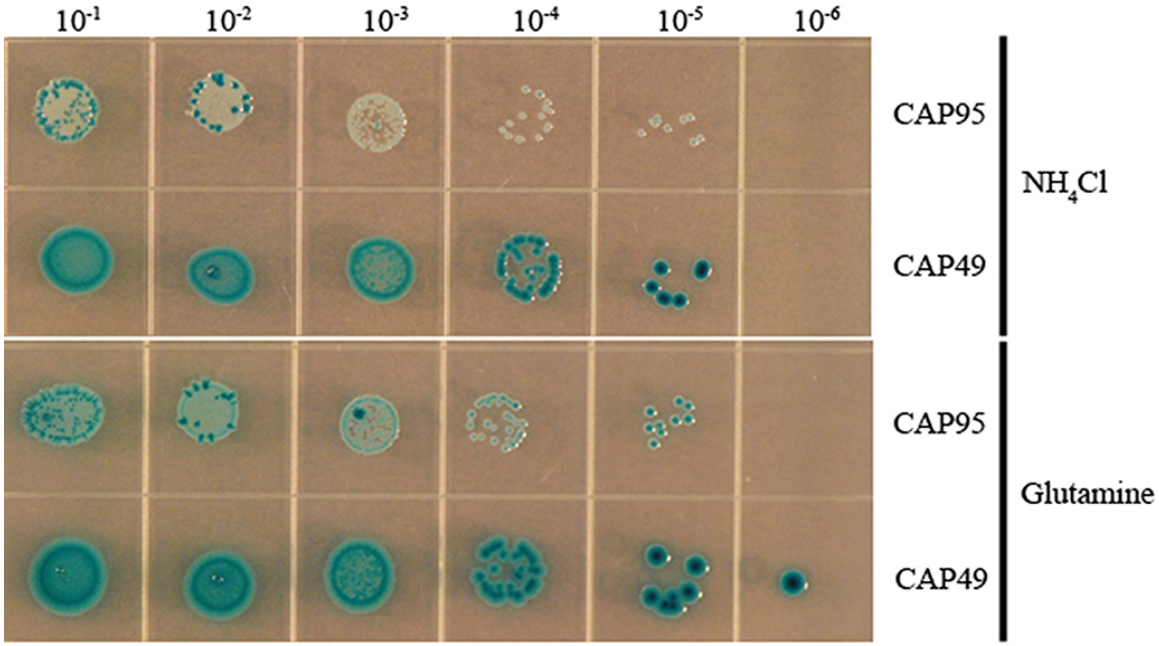

Figure 3.10 Glutamine relieves SMCR in an over-repressed strain. Colonies from M9 0.4% glycerol plate of strain CAP95 (*hpr*S53A) or CAP49 (wild-type *hpr*) were resuspended in carbon-free M9. The suspension was washed twice in carbon-free M9, then resuspended to an OD_{595} 0.1. Serial 10-fold dilutions were made 5 μL of the indicated dilution was spotted on M9 0.05% succinate, 0.1% lactose, X-gal, with or without 0.2% glutamine.

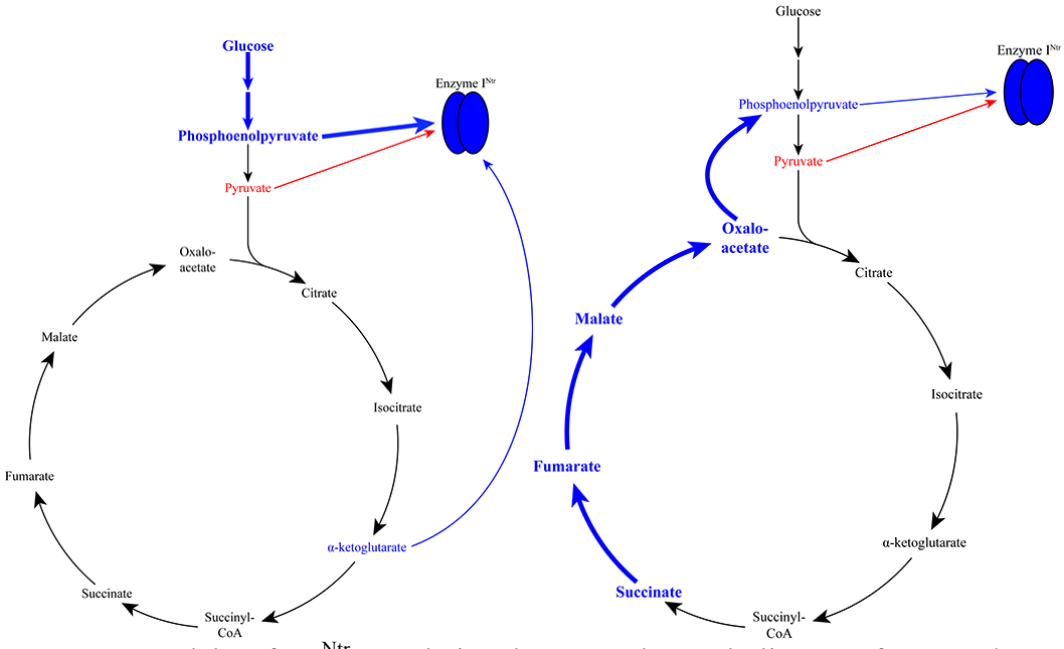

Figure 3.11 Models of EI^{Ntr} regulation by central metabolism. Left, *E. coli* central metabolism during growth on glucose; right, *S. meliloti* central metabolism during growth on succinate. In the case of *E. coli*, where glucose is the preferred carbon source, the [PEP]:[pyruvate] ratio represents flux through glycolysis. The concentration of α-ketoglutarate in the cell represents the levels of TCA intermediates, which is an intertwined, but separate system from glycolysis. While *S. meliloti* grows on succinate, its preferred carbon source, the [PEP]:[pyruvate] ratio is set by the gluconeogenic flux departing the TCA cycle. With α-ketoglutarate only two steps removed from succinate it represents the same overall levels of TCA carbon, making its detection by EI^{Ntr} redundant.

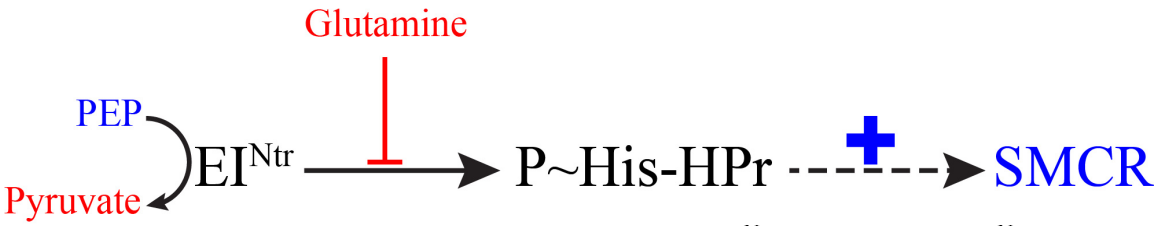

Figure 3.12 Model depicting regulation of SMCR by EI^{Ntr} in *S. meliloti*. EI^{Ntr} measures the intracellular carbon and energy status using the ratio of [PEP]:[pyruvate]. It integrates nitrogen availability through inhibition by glutamine. Conditions that increase EI^{Ntr} phosphorylation of HPr-His (depicted in blue) strengthen SMCR, while decreases in activity (depicted in red) weaken SMCR.

Chapter 4
Dephosphorylation of HPr

Characteristics of HPr. The second protein in the PTS is the diminutive (typically 9-10 kDa) protein HPr. Originally called the heat resistant protein, due to its method of purification from *E. coli*, it is more commonly referred to as the histidine containing protein (85, 153). Structurally, HPr is an open β-sandwich protein containing a four-strand β-sheet and three α-helices (154). This topology has been seen in all solved HPr structures despite relatively low sequence conservation (153). The interaction between HPr and all of its partners occurs at a single face of the protein. There are a number of residues that are highly conserved or invariant in all HPr sequences (the numbering used will be based on the *E. coli* HPr). The active site histidine-15 is invariant in HPr, as is the nearby arginine-17. Serine-46, which is phosphorylated by HPrK in Gram-positive bacteria, is present even in the HPr of species that lack HPr kinase. Glycines 13, 58, and 67 are all invariant, as is glutamate-83. Mutation of arginine-17 causes a decrease in the V_{max} and an increase in the K_m, with the severity depending on the exact mutation (155).

Until recently, HPr in Gram-negative bacteria was seen largely as a passive player in cellular homeostasis, responsible for the transfer of phosphate, but not direct regulation of other systems. The first interaction partner found for HPr was *E. coli* glycogen phosphorylase (GP) (156). Dephospho-HPr binds to GP with a high affinity and this binding is also highly specific as NPr does not bind GP, nor does HPr bind GP from mammals. Binding of HPr to GP increases its activity 2.5-fold. Recently, it was also shown that dephospho-HPr in *E. coli* binds Rsd, which is an anti-sigma factor that alters

the selectivity of the core RNA polymerase for σ^{70} (157). HPr reduces the affinity of Rsd for σ^{70}, allowing it to bind RNA polymerase and delaying the switch to σ^{S}. In *Vibrio vulnificus*, dephospho-HPr stimulates the activity of pyruvate kinase A (PykA) in a P_i dependent manner (158). Stimulation of PykA by HPr increases the carbon flux through the final step of glycolysis and into the TCA cycle. Taken together, these interactions show that HPr is not the passive intermediate that it was once believed to be. While we do not have direct evidence of HPr playing an active role in *S. meliloti*, there is an indication that this is the case. While single deletions in either *manX* or *ptsN* cause an overrepressed phenotype, deletion of both *manX* and *ptsN* appears to be lethal. However, the triple *hpr manX ptsN* mutant can be isolated (unpublished results). This implies that excess P~His-HPr is toxic to the cell, possibly due to interaction with an unknown regulatory system.

Dephosphorylation of HPr. As opposed to phosphoserine (and the other phosphoester amino acids), phosphohistidine and phosphoimidazole are chemically unstable species (159). In addition to the high ΔG^0 of hydrolysis (-12 to -14 kcal mol^{-1}), phosphoramidate amino acids are acid-labile (160, 161). Early experiments with *E. coli* HPr showed that its rate of phosphohydrolysis was greater than that of 1-phosphohistidine (162). Phosphorylated histidine of HPr has an elevated pk_a of 7.8 compared to 7.0 for free phosphohistidine (163, 164). High rates of P~His-HPr hydrolysis have also been measured in *Staphylococcus aureus*, *Streptococcus salivarius*, and *Enterococcus faecalis* (126, 165, 166).

A number of residues have been implicated in the high rate of P~His-HPr hydrolysis. Replacement of the invariant arginine-17 with any other amino acid

(including the chemically similar lysine) dramatically reduces the rate of autodephosphorylation (155). Urea denatured wild-type HPr and the R17G mutant dephosphorylate at the same rate, which indicates that the phosphohydrolysis rate is dependent on the tertiary structure of the protein. Deletion of glutamate-85 decreases the spontaneous dephosphorylation rate by 25%, while mutation of the reside to lysine shifts the pH-dependence of hydrolysis so that the maximum rate is 2 pH units lower (167). The conservative D69E site-directed mutant undergoes spontaneous phosphohydrolysis at approximately half the rate of the wild-type protein (168).

Saturation of incomplete PTS. Unlike the carbohydrate-type systems, incomplete phosphotransferase systems have no obvious phosphate sink. In order for a PTS to remain sensitive to changing conditions it must be able to rapidly change the phosphorylation state of its proteins, including from the phosphorylated to unphosphorylated state. Based on our model, the transition from succinate to a secondary carbon source requires dephosphorylation of the PTS proteins. If the proteins remain phosphorylated then the secondary catabolic operons would be constitutively repressed and the cells would not be able to exit diauxic lag. This chapter describes how the HPr of *S. meliloti*, and likely other related α-proteobacteria, rapidly dephosphorylates after phosphorylation by EI^{Ntr}. This rapid phosphohydrolysis could maintain the sensitivity of the PTS as the availability of extracellular carbon changes, allowing for relief of SMCR in the absence of succinate and induction of secondary catabolic operons.

Results

***S. meliloti* HPr rapidly dephosphorylates at physiological pH.** While developing the native-PAGE assay for HPr phosphorylation we noticed that the protein would dephosphorylate during electrophoresis (Fig. 4.1). The hydrolysis appeared to be pH-dependent and below pH 9 there was always smearing between the P~HPr and dephosphorylated HPr bands. This necessitated the use of a high pH running buffer to measure HPr phosphorylation, but it also indicated that P~HPr might dephosphorylate at an unusually high rate. To rule out a contribution from the buffering system, and to approach this phenomenon quantitatively, the phosphohydrolysis of HPr was measured using a modified LDH (126). In the modified assay, EI^{Ntr} is added to the reaction (pH 7.5 at 30°C) at 1 μM, resulting in complete phosphorylation of HPr within 10 s. Due to the high concentration of EI^{Ntr} in the reaction dephosphorylation of HPr becomes the rate-limiting step, which is detected by the decrease in the A_{340}. The rate of HPr phosphohydrolysis was measured at concentrations ranging from 10-50 μM and the data were fit using linear regression. The pseudo-first order rate constant was calculated as 0.47 min^{-1} (Fig. 4.4), approximately 5-fold faster than *E. coli* P~HPr, which was measured at 37°C.

Identification of an HPr residue involved in autodephosphorylation. I predicted that increased phosphohydrolysis could be a characteristic of HPr from incomplete PTS. Since α-proteobacteria primarily contain incomplete PTS, while γ-proteobacteria primarily contain complete PTS, there should be sequence characteristics that are responsible for the difference in rates that are conserved within these classes (94, 169). A

MUSCLE alignment of HPr sequences revealed that the α-proteobacteria have a conserved arginine at residue 19 (*S. meliloti* numbering) that is absent from the γ-proteobacteria homologs (Fig. 4.2). As mentioned above, arginine-17 of the *E. coli* HPr contributes to its elevated phosphohydrolysis relative to free phospho-histidine. In order to explore the contribution of this residue to phosphohydrolysis an HPr arginine-19 to leucine site directed mutant was made (leucine being the most common amino acid at this position in γ-proteobacteria).

Spontaneous phosphohydrolysis is diminished in HPr(R19L). The HPr(R19L) mutant was expressed as a his_6-tagged fusion and purified using the same protocol as wild-type HPr. The culture yield (measured in pellet wet weight) of cultures expressing HPr(R19L) was approximately twice that of those expressing wild type HPr (data not shown). This may be a result of the expressed protein interacting with the native PTS. Deletion of PTS genes results in increased biomass of *E. coli* W3110, so interference of the native PTS by HPr(R19L) could be the root cause of the increased culture yield (170). Phosphorylation of HPr(R19L) by EI^{Ntr} was kinetically characterized and found to be nearly identical to wild-type HPr (Fig. 4.3). The calculated K_M of EI^{Ntr} for HPr(R19L) was 13.3±1.2 μM and the k_{cat} was 1.08±0.3 s^{-1}, which are 104% and 97% of the wild-type constants, respectively. Since the kinetic constants were so similar to the wild-type protein, the same modified LDH assay was used to measure spontaneous dephosphorylation of HPr(R19L). The rate constant calculated for the site-directed mutant was found to be 0.22 min^{-1}, which is approximately half the rate of wild-type *S. meliloti* HPr (Fig. 4.4).

Discussion

In the canonical PTS, sugar import represents a built-in sink for phosphate introduced to the system. Due to the structure of incomplete PTS, specifically the lack of membrane transport proteins, there is no comparable output for phosphate derived from PEP. If the PTS were incapable of draining phosphates from the system then it would rapidly saturate, becoming locked in the repressive state. To maintain sensitivity to changing environmental conditions, there must be a method to dephosphorylate the proteins in an incomplete PTS. In Gram-positive bacteria the phosphate bound to HPr-Ser is enzymatically removed, typically by the phosphorylase activity of HPrK/P. *Mycoplasma pneumoniae* has an alternative method for HPr-Ser-P dephosphorylation. In this system the PP2C-type phosphatase PrpC hydrolyzes HPr-Ser-P in response to inorganic phosphate and glycerol-2-phosphate (171). To our knowledge, there are no reports of enzymatic dephosphorylation of HPr-His~P or EIIA~P in incomplete PTS. Bacteria with additional carbohydrate PTS may be able to circumvent this problem through cross talk with the parallel system. The phosphate could be transferred onto proteins that can drain it through sugar phosphorylation. Organisms such as *S. meliloti* have no carbohydrate PTS, and must have a dedicated method for removing phosphate from the system. While this problem has been referenced in work on incomplete PTS there is no published work investigating a solution.

While developing the native-PAGE assay for HPr phosphorylation we noticed that P~HPr could only be resolved on very alkaline gels. This was curious, since P~HPr has been detected using Tris/glycine systems with pH values below 9 (126, 157). While analyzing a MUSCLE alignment of HPr sequences from various bacteria it was noticed

that in α-proteobacteria, which generally contain only an incomplete PTS, there was a conserved arginine at position 19 (*S. meliloti* numbering) near the phosphorylated histidine. This arginine is notable because basic amino acids are known to destabilize phosphohistidines and another nearby arginine in HPr specifically contributes to the protein's high rate of spontaneous dephosphorylation (155).

Measurement of the phosphohydrolysis rate of *S. meliloti* HPr at pH7.5 showed that spontaneous dephosphorylation occurs at a very high rate, even compared to HPr from other bacteria. Replacement of arginine-19 with leucine caused an approximately 2-fold decrease in the rate of dephosphorylation. Since the kinetic constants for HPr(R19L) phosphorylation by EI^{Ntr} is nearly identical to that of the wild-type protein the decreased rate is not likely due to an artifact of the LDH assay. Replacement of arginine-17 in *E. coli* with the chemically similar lysine causes not only a large decrease in phosphydrolysis rate, but also caused a defect in the kinetics of HPr phosphorylation by EI. This implies that while the invariant arginine is involved in both dephosphorylation and phosphotransfer activity (both of which are possibly intertwined), arginine-19 of *S. meliloti* HPr is not required for phosphorylation, but does affect autodephosphorylation.

Considering the conservation of arginine-19 among α-proteobacteria with incomplete PTS we believe that increased autodephosphorylation prevents accumulation of phosphate within the system. Without an active mechanism for removing phosphate from the PTS the proteins must have evolved a mechanism to prevent saturation. Low stability of phosphate in the system would require continual EI^{Ntr} activity, which would maintain the sensitivity of the system to changing environmental conditions. Maintaining a dynamic system ensures that the PTS would remain sensitive to small fluctuations in

the metabolic state of the cell. While the overall rate of dephosphorylation is small relative to the k_{cat} of EI^{Ntr}, these processes are not occurring in isolation. Glutamine is one of the most abundant metabolites within bacteria, and should always be present in concentrations high enough to reduce EI^{Ntr} activity. In Gram-positive bacteria, P-Ser-HPr either cannot be phosphorylated by EI, or is a poor substrate for the enzyme. Assuming this holds true in *S. meliloti*, the activity of HPrK would further reduce HPr-His phosphorylation by EI^{Ntr}. We have been unsuccessful in purifying soluble and active HPrK, but genetic data support this model (both *hprK* and *hpr*S53A alleles are overrepressed, indicating excessive phosphorylation of HPr-His). Taken together, these indicate that EI^{Ntr} activity within the cell will be greatly reduced to its rate *in vitro*, possibly to a level that matches HPr dephosphorylation. To assess the impact of the R19L mutation *in vivo*, we are currently building a strain that will express the protein in a Δ*hpr* background.

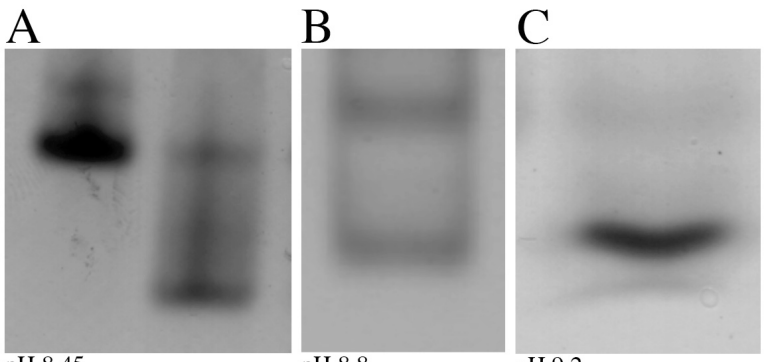

Figure 4.1 Hydrolysis of P~HPr observed during electrophoresis. A, Tris/Tricine pH8.45; B, Tris/glycine pH8.8; C, Tris/CAPS pH9.2. Reactions were set up under conditions expected to result in completely phosphorylated HPr. When P~HPr was run on polyacrylamide gels below pH9 the bands smear upwards due to dephosphorylating during electrophoresis.

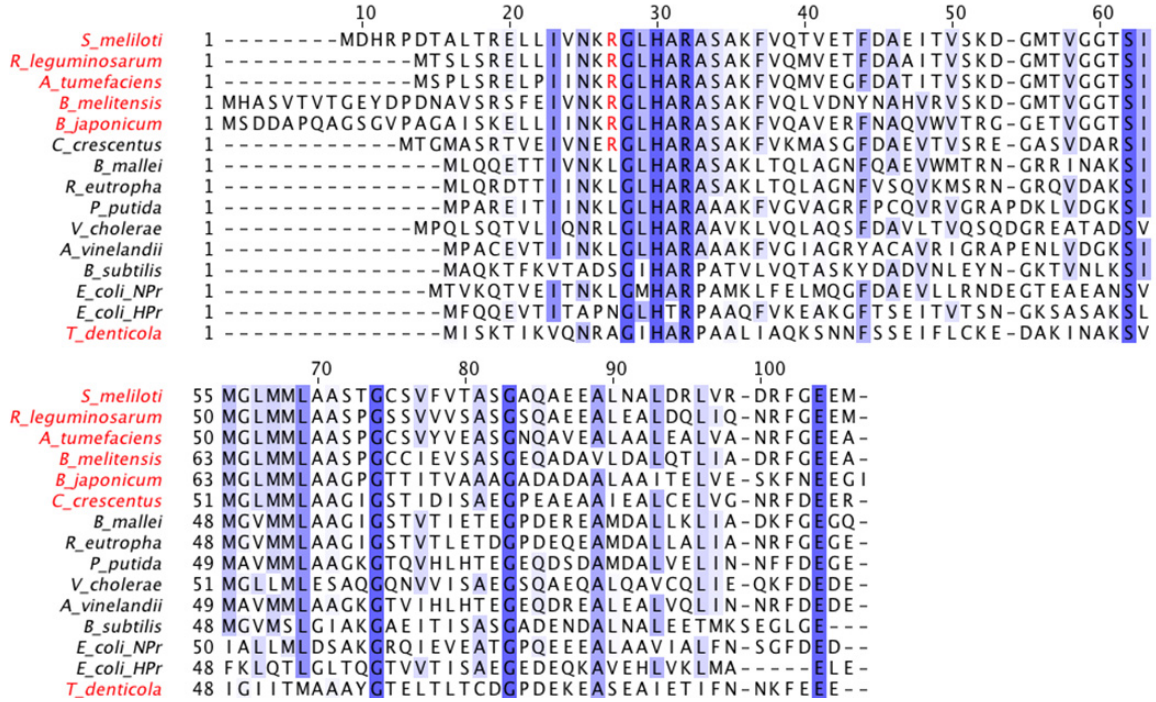

Figure 4.2 MUSCLE Alignment of HPr sequences. Names that are highlighted red represent bacteria that only contain incomplete PTS. The arginine that is enriched in α-proteobacteria is also highlighted red. The phosphorylated histidine is at position 30 of the alignment, and the invariant arginine is at position 32.

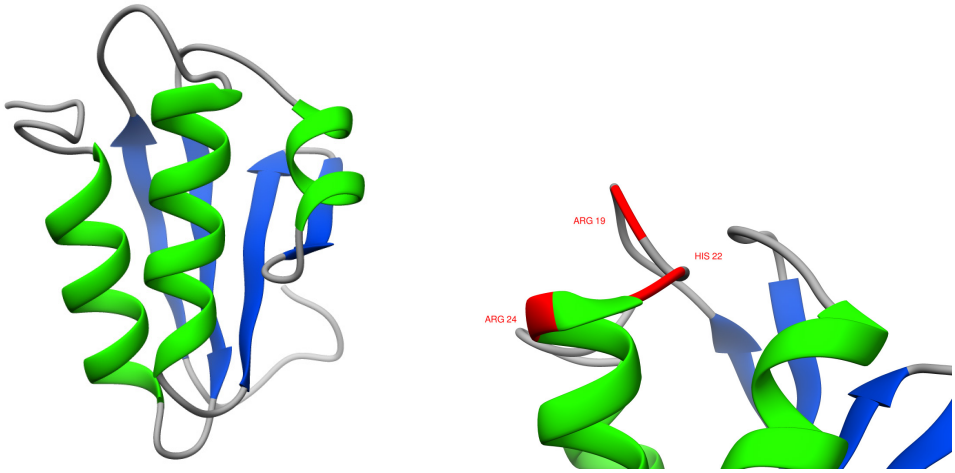

Figure 4.3 Predicted structure of *S. meliloti* HPr. The structure was predicted by submitting the complete protein sequence to the Phyre[2] homology web server (172). Left, depiction of the entire HPr structure showing the β-sandwich fold. Right, close up of the histidine active site. Highlighted in red are: arginine-19; histidine-22, which is the phosphorylated histidine; and arginine-24, which is equivalent to arginine-17 in *E. coli* HPr.

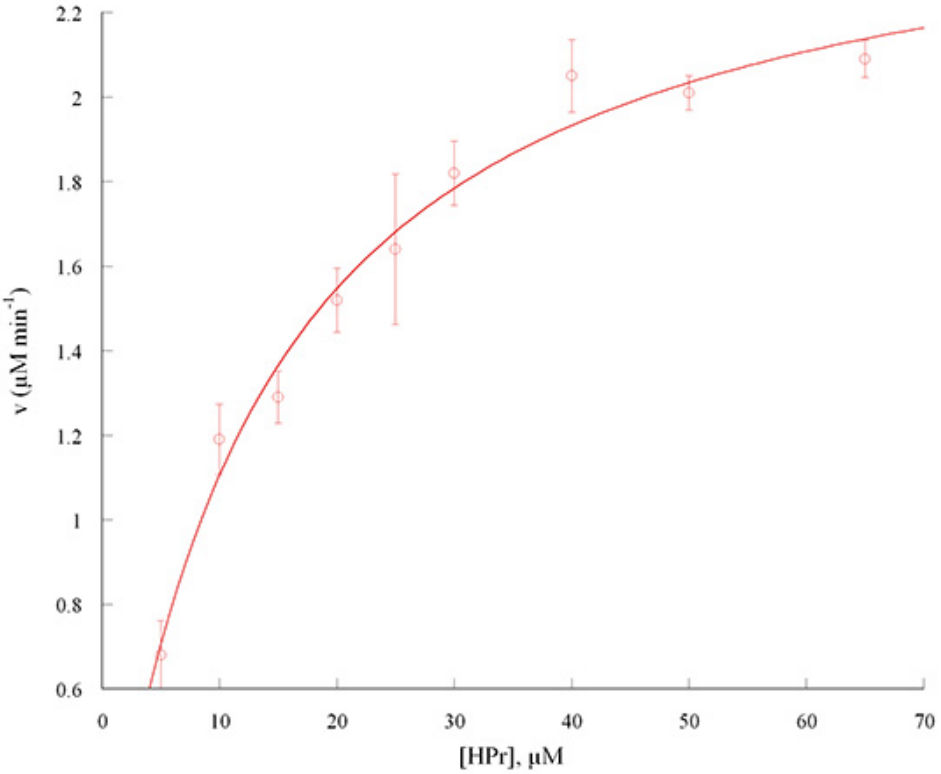

Figure 4.4 Phosphorylation of HPr(R19L) by EI^{Ntr}. Reactions were performed using the same method as wild-type HPr. Data points are the mean of three replicates and error bars represent the standard deviation. The line represents a fit of the data to the Michaelis-Menten equation.

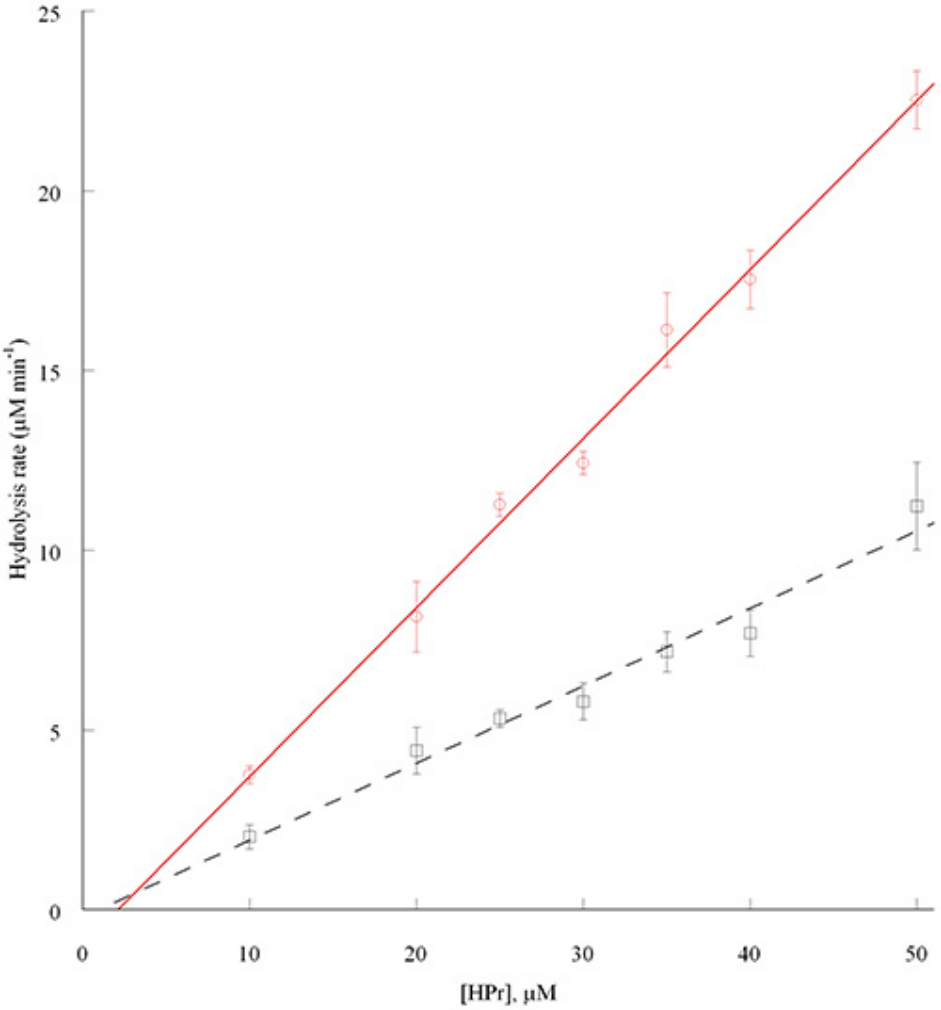

Figure 4.5 Spontaneous dephosphorylation of HPr and HPr(R19L). Dephosphorylation was measured using the LDH-coupled assay in 0.1M NaOAc, 1mM DTT, 10mM $Mg(OAc)_2$, 0.1M Na-HEPES pH7.4 with 1μM of EI^{Ntr}. Red, wild-type HPr; Black, HPr(R19L). Data points are the mean of three replicates and the error bars represent the standard deviation. The lines represent a linear fit to the data.

Chapter 5
Summary of Thesis

Outside of the canonical PTS models the system is poorly understood. The increased availability of genome sequences has revealed that many bacteria contain unusual PTS that are often involved in regulation, but not sugar transport. In the majority of α-proteobacteria not only are the majority of PTS regulatory, but also include an HPr kinase, which was traditionally believed to be restricted to Gram-positive bacteria. Incomplete PTS regulate a wide variety of systems that are typically tied to central metabolism. The PTS of *S. meliloti* fulfills the traditional role of regulating CCR, but it also regulates production of succinoglycan and PHB, and *hprK* and *ptsN* mutants are $Nod^{+}Fix^{-}$. In the closely related pathogen *B. melitensis*, the PTS exerts control over virulence. The PTS of the diazotrophic γ-proteobacterium *A. vinelandii* regulates PHB accumulation, alkylresorcinol synthesis and nitrogen fixation. It is clear that investigation of these non-canonical PTS is critical to understanding the physiology of bacteria that impact humans in a number of ways.

EI^{Ntr} is the first enzyme in the PTS, and its activity controls introduction of phosphate into the HPr-His arm of the pathway. Because EI^{Ntr} initiates the phosphorylation cascade its activity results in imposition of SMCR. In order to understand how SMCR is regulated in *S. meliloti*, EI^{Ntr} was characterized biochemically. Carbohydrate-type Enzymes I that have been characterized in other bacteria phosphorylate their respective HPr at very high rates, often approaching the diffusion limit. EI^{Ntr} from *S. meliloti* diverges from this trend, phosphorylating HPr at a rate that is approximately 10^4 fold slower. This is still 10-fold faster than the published rate of NPr

phosphorylation by *E. coli* EI^{Ntr}, although this difference may be due to inherent flaws in the methods used for purification and activity measurements. Carbohydrate-type PTS are responsible for import of sugars from the environment and, by extension, the growth rate of an organism. From this it is clear that a high rate of EI activity is beneficial to an organism, allowing bacteria such as *E. coli* to maintain high growth rates when ample sugar is available. Incomplete PTS do not directly participate in carbon uptake, and instead serve a regulatory role. The rapid phosphorylation observed in their carbohydrate counterparts is therefore unnecessary to their function, and could potentially lead to a detrimental over saturation of the PTS components.

When glutamine was added to HPr phosphorylation reactions, a marked decrease in the fraction of P~HPr was observed. The inhibitory effect of glutamine on EI^{Ntr} was confirmed using the LDH-coupled continuous assay. Inhibition of EI^{Ntr} occurred even at micromolar concentrations of glutamine, which is one of the most abundant metabolites within bacterial cells. In most proteobacteria the overall nitrogen status of the cell is detected through the ratio of glutamine to α-ketoglutarate. The glutamine sensitivity of EI^{Ntr} shows that carbon regulation in *S. meliloti* is intimately coupled to nitrogen availability. Since α-ketoglutarate activates EI^{Ntr} of *E. coli*, and also serves as a signal for TCA balance in a number of regulatory systems, its affect on EI^{Ntr} activity was assayed. When α-ketoglutarate was added to HPr phosphorylation reactions it did not change the fraction of P~HPr. Another possibility was that α-ketoglutarate could alleviate glutamine inhibition by competing for EI^{Ntr} binding. When α-ketoglutarate was added to phosphorylation reactions that contained glutamine it did not relive inhibition of EI^{Ntr}. In *E. coli,* sensitivity to α-ketoglutarate provides additional information regarding TCA

cycle balance to EI^{Ntr}, the activity of which is determined by the [PEP]:[pyruvate] ratio. During growth of *S. meliloti* on its preferred carbon source succinate derives both PEP and pyruvate from gluconeogenesis. During gluconeogenic growth, the carbon backbone of both PEP and pyruvate is derived from TCA cycle precursors. In this case, succinate and α-ketoglutarate both represent TCA cycle levels, making sensation of α-ketoglutarate redundant.

In this work, the binding of glutamine by the GAF domain of EI^{Ntr} was measured using ITC. The binding studies revealed that the GAF domain binds glutamine with an affinity of 35μM. No binding could be measured when α-ketoglutarate was titrated into the GAF domain, confirming that EI^{Ntr} is insensitive to this metabolite. *S. meliloti* EI^{Ntr}, *E. coli* EI^{Ntr}, and *A. vinelandii* NifA all share a conserved phenylalanine in the GAF domain. The EI^{Ntr}(F102S) site-directed mutant is not inhibited by the addition of glutamine to an assay, indicating that F102 is important for ligand binding.

During optimization of native-PAGE phosphorylation assays I noticed that HPr dephosphorylated during electrophoresis, with the highest rates of phosphohydrolysis occurring in neutral pH gel buffers. This effect could only be avoided when the gel was buffered at a pH exceeding 9. While hydrolysis of the phosphoramidate bonds is known to occur in both P~His and *E. coli* P~His-HPr, it appeared to occur at an elevated rate in *S. meliloti* P~HPr. Spontaneous phosphohydrolysis of *S. meliloti* P~HPr occurs at a rate of 0.47 min^{-1}, which is approximately 5-fold faster than the reported rate of *E. coli* HPr. The HPr of α-proteobacteria with only an incomplete PTS have a conserved arginine near the phosphorylated histidine, while leucine is the most common residue at this position in bacteria with complete carbohydrate-type phosphotransferase systems. This arginine is

noteworthy because arginine-17 of the *E. coli* HPr, which is also situated near the active site histidine, is responsible for the elevated phosphohydrolysis rate relative to free phospho-histidine. A site-directed HPr(R19L) mutant was constructed and expressed. The k_{cat} and K_M for EI^{Ntr} phosphorylation of HPr(R19L) are 97% and 104% of the values for wild type HPr, respectively. These values are within experimental variation, implying that arginine-19 is not involved in the HPr-EI^{Ntr} association, nor is it involved in the transfer of phosphate from EI^{Ntr} to HPr. Spontaneous phosphohydrolysis of the R19L mutant occurs at 0.22 min^{-1}, which is about 2-fold lower than the wild type protein, and a little more than twice the rate of *E. coli* HPr. This implies that while arginine-19 plays an important role in maintaining a high rate of autodephosphorylation, there are likely other sequence characteristics responsible for the elevated rate in *S. meliloti*.

The conservation of arginine-19 within α-proteobacteria with only an incomplete PTS implies that HPr from these bacteria also undergo rapid autodephosphorylation. This implies that P~His-HPr instability is integral to the proper function of these regulatory PTS. Since incomplete PTS are not responsible for sugar phosphorylation they must have an alternate means of draining phosphate from the system. These bacteria may have solved the phosphate saturation problem through rapid phosphohydrolysis of P~His-HPr. Because the phosphate within the system is so unstable, the fraction of phosphorylated HPr would need to be maintained by the activity of EI^{Ntr} in state of equilibrium. The arginine-19 to leucine mutation of HPr stabilizes histidine phosphorylation, but is not compromised as a substrate for EI^{Ntr}, implying that the adaptation is specifically related to stability of the phospho-proteins. This system would be very sensitive to changes in the environment, where small shifts in the activity of EI^{Ntr} would be immediately

translated to changes in the phosphorylation state of the PTS proteins. Perturbations to central metabolism would be propagated through the PTS without the need for additional proteins required for dephosphorylation of HPr or either EIIA.

The work presented here explores the dynamic nature of the incomplete phosphotransferase system of *S. meliloti*. Enzyme I^{Ntr}, the first protein in the PTS, integrates signals representing the carbon, nitrogen, and energy status of the cell. Propagation of these signals through the PTS allows the cell to fine tune its physiology for optimal growth in the environment. The GAF domain of EI^{Ntr} is responsible for sensing these signals within the cell, and its sensitivity to metabolites appears to be specific for the organism's particular needs. While EI^{Ntr} controls the introduction of phosphate into PTS it appears that HPr is responsible for preventing oversaturation. The instability of P~His-HPr prevents phosphate overflow, maintaining the sensitivity of the system during the transition from growth on succinate to a secondary carbon source.

Appendix

Introduction

While exogenous glutamine weakens SMCR, this phenomenon was also observed when glutamate (which does not affect EI^{Ntr} activity) was added to the medium. One explanation for this observation is that interconversion of glutamate and glutamine results in elevated intracellular glutamine concentrations during growth. This section details attempts to resolve this discrepancy through physiological experiments that ultimately proved inconclusive. These experiments attempted to measure the strength of SMCR in a time scale shorter than that required for accumulation of glutamine. The first portion of the appendix focuses on modification of diauxic growth curves designed to measure the effect of added glutamine during the transition from succinate to raffinose. The remainder focuses on measurement of inducer exclusion using whole-cell α-galactosidase assays. Decreased inducer exclusion should be the first step in the relief of SMCR, and therefore will be the most immediate effect of succinate exhaustion.

Results

The effect of amino acids on diauxic growth. Growth of strain Rm1021 in media containing succinate, raffinose, and amino acids such as glutamate, asparagine, and alanine also results in a decreased diauxic lag (Fig. A.1 and A.2). Since these amino acids to not inhibit EI^{Ntr} like glutamine, this effect is either due to increased intracellular glutamine concentrations, or implies that the reduced diauxic lag in the presence of

glutamine is a general phenomenon unrelated to EI^{Ntr} activity. In contrast, addition of methionine causes a dramatic increase in the diauxic lag (Fig. A.3). While this is an interesting phenomenon, we could not determine the mechanism and was not studied further. For the experiments detailed in this section optical density and fluorescence measurements were collected as above. To measure the strength of SMCR on a short time-scale glycerol grown cultures of strain Rm1021 were inoculated into flasks of M9 with 0.1% succinate at an initial OD_{595} of 0.02. The succinate cultures were grown at 30°C until they reached mid-log phase, then were diluted 10-fold into M9 with 0.1% raffinose and the 0.05% of the indicated amino acid in 48-well plates. Addition of glutamine, glutamate, and asparagine decreased the lag time after dilution into raffinose. Interestingly, the lag phase for medium without an amino acid added lagged for 40 h before growth on raffinose commenced, which is considerably longer than the normal diauxic lag.

Development of an inducer exclusion assay. An assay for inducer exclusion was developed based on the prediction that in raffinose grown *S. meliloti,* which have a fully induced *melA-agp* operon, inducer exclusion should cause transport of α-galactosidase substrates to become the rate-limiting step. The α-galactoside analog *p*-nitrophenyl-α-D-galactopyranoside (αPNPG) is hydrolyzed by α-galactosidase, releasing *p*-nitrophenol, a compound that absorbs strongly at 415 nm. Inducer exclusion imposed by succinate exposure should result in a decrease in αPNPG hydrolysis rates by whole cells. In all of the experiments described within this section strain Rm1021 was grown to mid-log phase in M9 0.4% raffinose, which will result in strong induction of the *melA-agp* operon. The cells were then harvested by centrifugation, washed in M9 without carbon to remove

unmetabolized raffinose that could compete with αPNPG for uptake, and resuspended in the same.

To determine if inducer exclusion could be measured using this method the washed cells were diluted into M9 containing the indicated concentration of succinate and were then incubated at 30°C for 1.5 hours. Cells were then washed, resuspended in M9 with the same concentration of succinate plus 1 mM α-PNPG, and the α-galactosidase activity was measured by the change in absorbance at 415 nm (Fig. A.4). αPNPG hydrolysis was reduced in cells incubated with succinate in a concentration dependent manner. To determine the optimal succinate incubation time for establishing inducer exclusion the raffinose-grown cells were diluted into M9 0.4% succinate, and incubated at 30°C. Cell aliquots were taken at the indicated time points and the αPNPG hydrolysis rate was measured immediately (Fig. A.5). In this experiment the rate of αPNPG hydrolysis was corrected using total cell protein measured with the Bichinchoninic (BCA) assay (Pierce). These data show that while incubation of the cells in the presence of succinate is reducing the αPNPG hydrolysis rate, the time taken to establish inducer exclusion was longer than expected. I reasoned that the long incubation time needed for succinate to take affect was due to low expression of *dctA*, which is an inducible transporter. To eliminate the lag time before inducer exclusion, induction of *dctA* would have to occur before succinate exposure. During the next experiment the raffinose starter culture was split in half and 20 mM maleic acid, a strong inducer of the *dct* system (173), was added to one flask. The cultures were incubated for an additional hour, and then harvested and washed as above. In the absence of succinate, pre-induced cells did not exhibit altered αPNPG hydrolysis, however, addition of 25 mM succinate

caused an immediate decrease in the hydrolysis rate (Fig. A.6). When pre-induced cells were mixed with 25 mM succinate and the αPNPG hydrolysis rate was measured, inducer exclusion could be observed during the kinetic measurement (Fig. A.7). Using this assay the effect of glutamine on inducer exclusion was measured. Addition of glutamine did not change the hydrolysis rate of αPNPG by whole cells (Fig. A.8). The lack of a detectable response towards glutamine may be a result of an inducible glutamine transporter that was not expressed during the course of these experiments. Alternatively, activation of EI^{Ntr} by succinate metabolism may overwhelm the inhibition caused by glutamine.

Discussion

The work described in this appendix explored the effect of amino acids on the strength of SMCR. The initial set of experiments used diauxic growth on succinate and raffionse to measure the strength of SMCR. With the exception of methionine, all of the amino acids tested reduced the length of diauxic lag to varying degrees. We still do not understand how methionine causes such a long diauxic lag. In the rhizobiales, the gene immediately downstream of the *hprK-manX-hpr* operon is *ahcY*, which encodes a protein involved in sulfur amino acid biosynthesis. No connection between AhcY and the PTS has been found, but this connection should be explored in the future. When succinate-grown cells were diluted into M9 raffinose there was a very long lag before growth commenced. Addition of the tested amino acids caused the culture to exit lag much earlier in the growth curve. This could be due to reduction of SMCR through inhibition of EI^{Ntr}, or if catabolism of amino acids is not repressed in the same was as α-galactosides, growth could have started using amino acids as a carbon source.

Without any success with diauxic growth I moved on to measuring inducer exclusion. I found that exposure to succinate reduced the hydrolysis of αPNPG in whole cells that were expressing the *melA-agp* operon. While succinate reduced the rate of αPNPG hydrolysis, it required more than an hour before the rate was substantially reduced. I believed this was due to low expression of *dctA* limiting the amount of succinate accumulating within cells. When *dctA* was induced by addition of maleic acid there was an immediate response to the addition of succinate. I had hoped that addition of glutamine would cause a decrease in inducer exclusion that could be detected using this assay, but unfortunately that was not the case. Addition of glutamine to cell suspensions had no affect on the reduction of αPNPG hydrolysis by succinate. It's unclear if the lack of a response was due to a lack of precision in the assay, if the cells did not take up glutamine, or if the added glutamine could not overcome the effect imposed by succinate. It appears that the best approach to studying the weakening of SMCR by glutamine is a genetic one. Since I have identified a residue in EI^{Ntr} that causes it to become glutamine blind a strain expressing only EI^{Ntr}(F102S) would need to be constructed. This is complicated by the extreme growth defect caused by deletion of *ptsP*, the gene that encodes EI^{Ntr}. Attempts to introduce *ptsP*(F102S) into *S. meliloti* before deleting the wild type gene locus were unsuccessful. Introduction of two copies of the wild type *ptsP* gene caused severe growth defects, and this was even worse in *ptsP* (F102S).

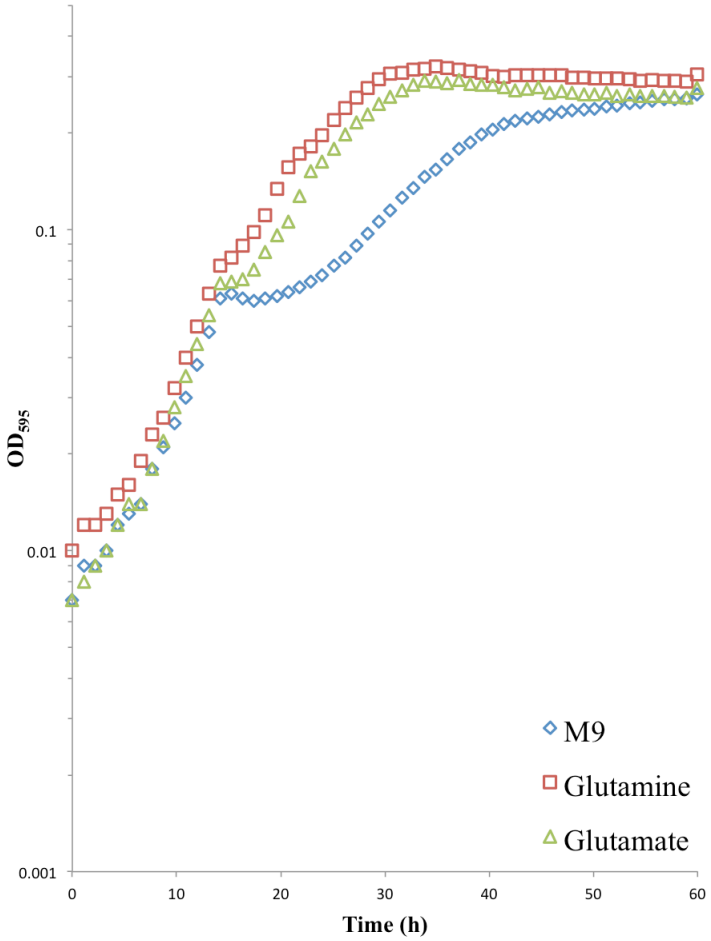

Figure A.1 Relief of SMCR by glutamine and glutamate. Strain Rm1021 was grown in M9 0.05% succinate, 0.1% raffinose, and 0.05% of the indicated amino acid.

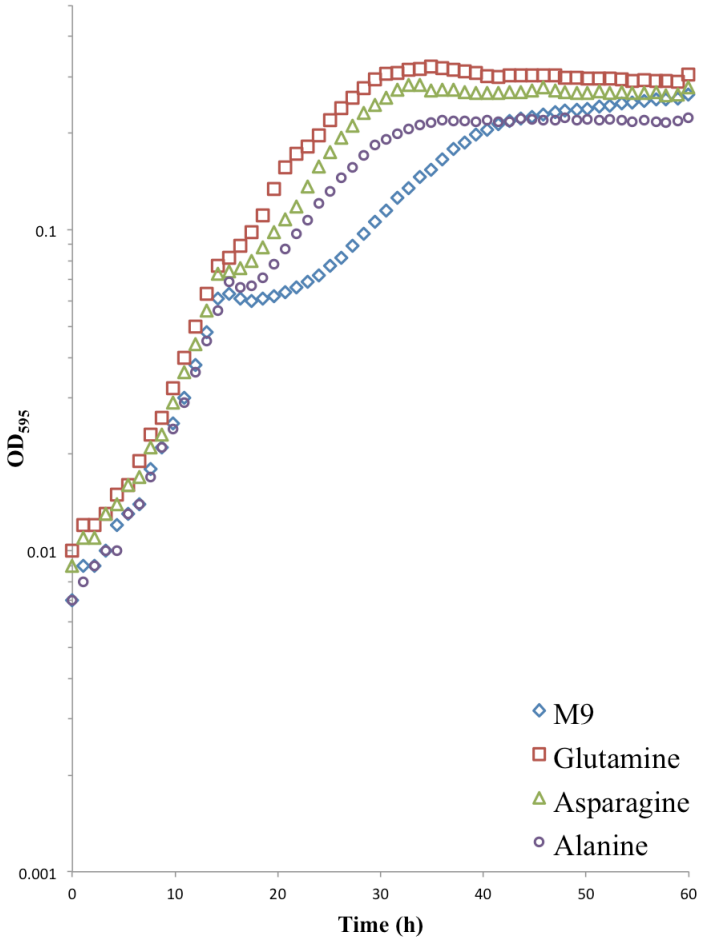

Figure A.2 Relief of SMCR by glutamine, asparagine, and alanine. Strain Rm1021 was grown in M9 0.05% succinate, 0.1% raffinose, and 0.05% of the indicated amino acid.

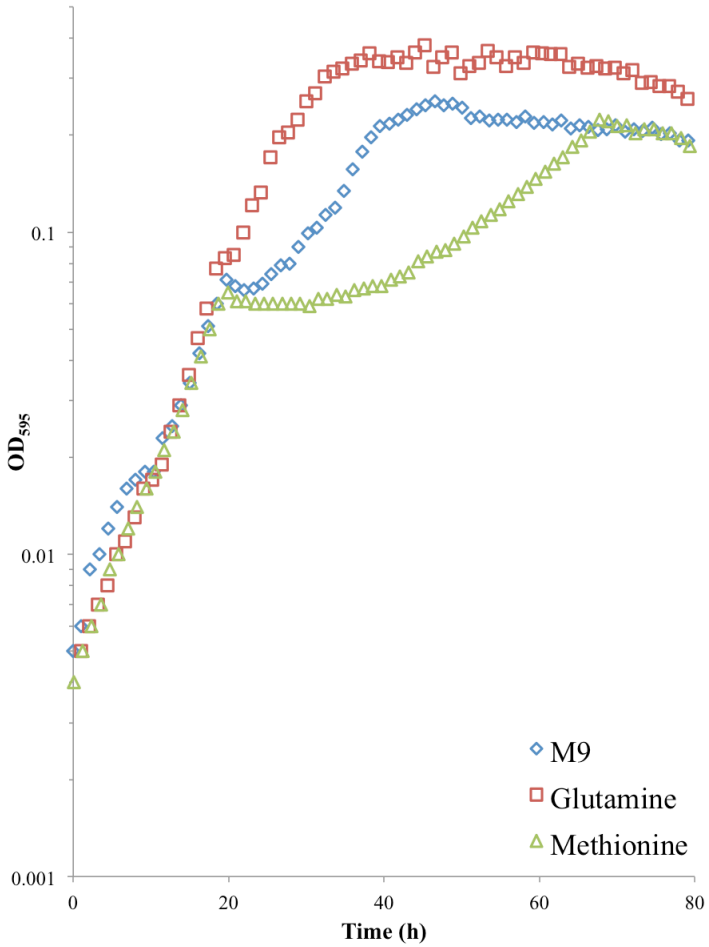

Figure A.3 Effect of glutamine and methionine on diauxic growth. Strain Rm1021 was grown in M9 0.05% succinate, 0.1% raffinose, and 0.05% of the indicated amino acid. The curves were shifted along the x-axis to align the point of succinate exhaustion.

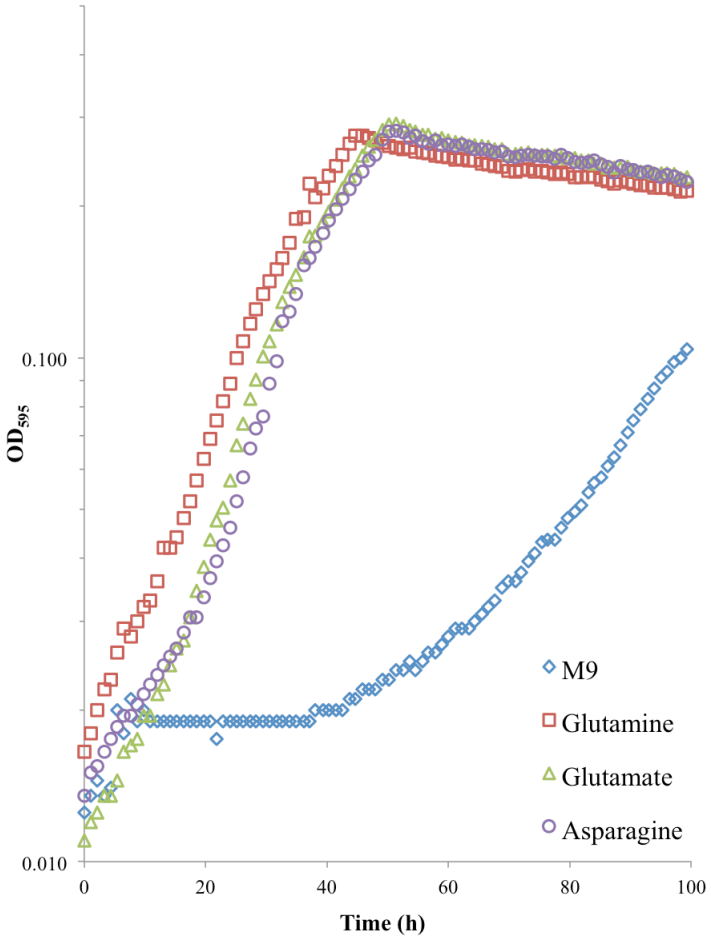

Figure A.4 Effect of amino acids on the exit from lag phase. Strain Rm1021 was grown to mid-log in M9 0.1% succinate, then diluted 10-fold into M9 0.1% raffinose and 0.05% of the indicated amino acid.

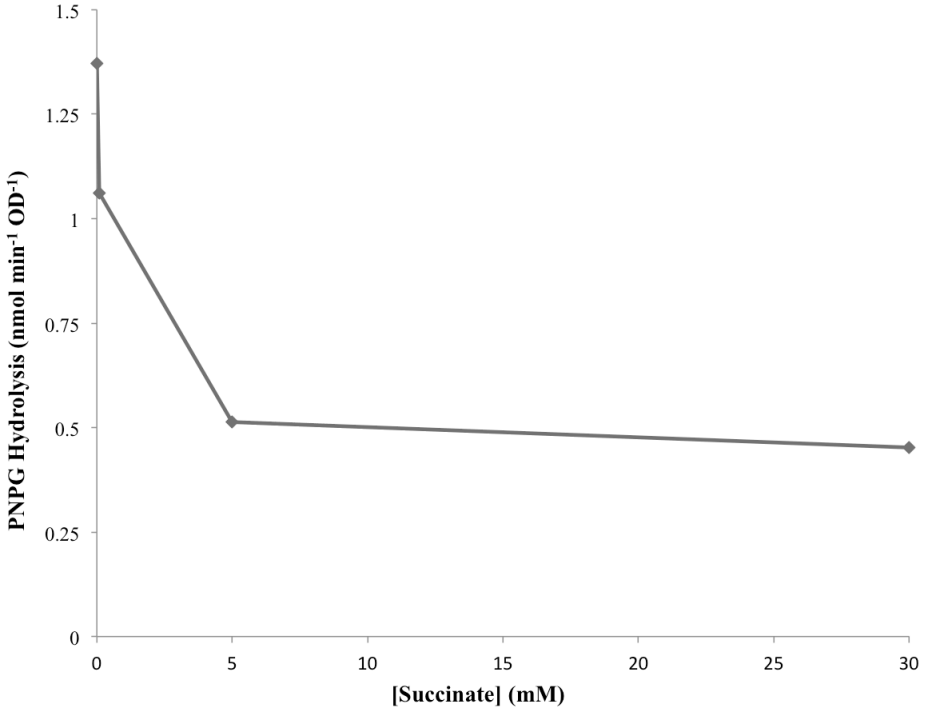

Figure A.5 Inducer exclusion measured by αPNPG hydrolysis. Raffinose grown cells were washed in carbon-free medium and incubated in the indicated concentration of succinate for 1.5 h. Rate of αPNPG hydrolysis was measured by A_{415}.

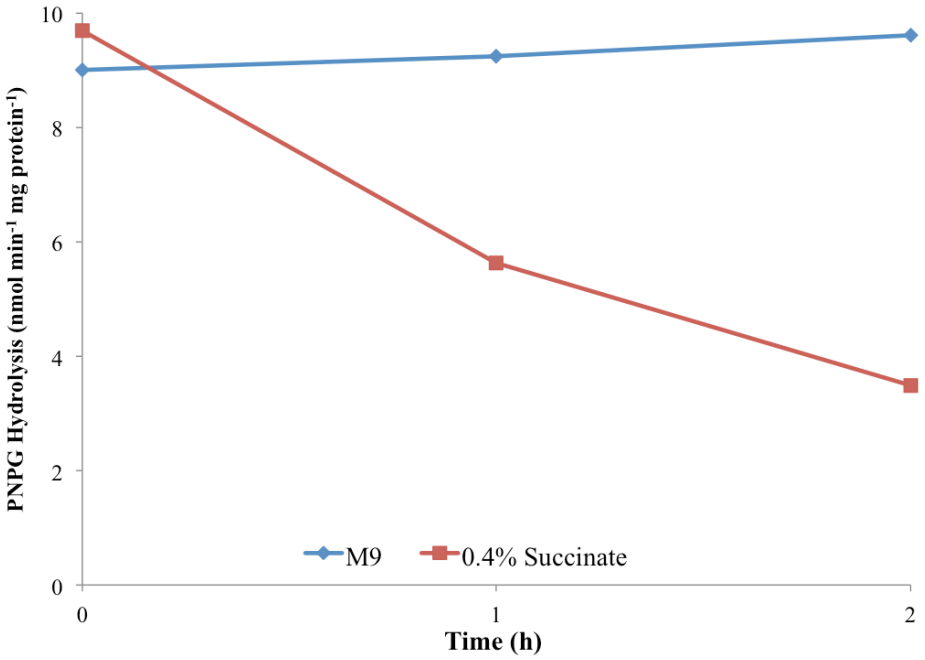

Figure A.6 The effect of succinate exposure time on αPNPG hydrolysis rate. Washed, raffinose grown cells were diluted into either M9 or M9 succinate and incubated at 30°C. Aliquots of cells were removed at the indicated time points and the rate of αPNPG hydrolysis was measured.

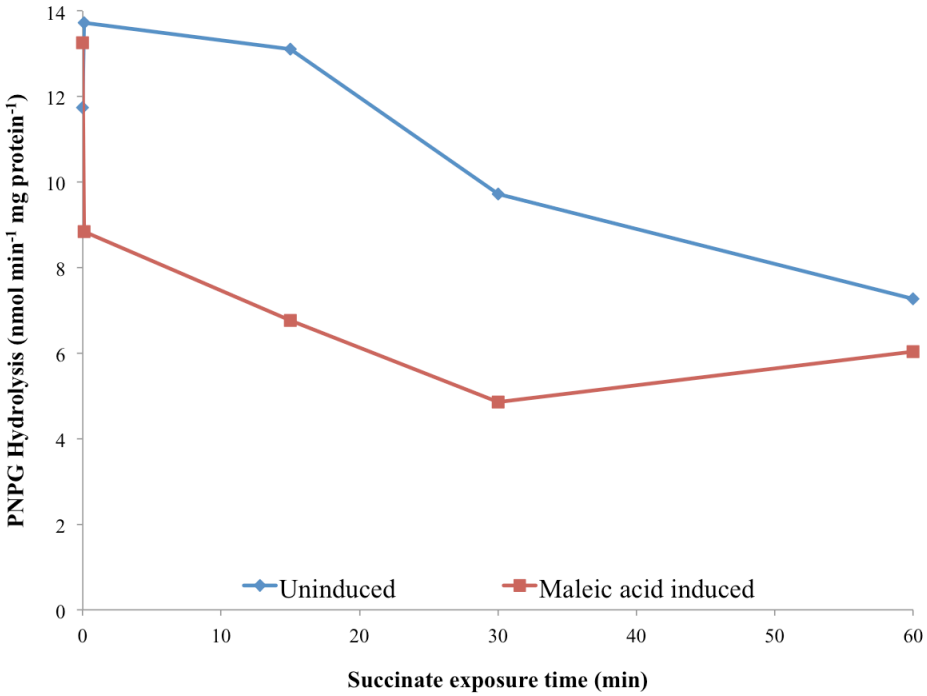

Figure A.7 Pre-induction of *dctA* before inducer exclusion assay. Strain Rm1021 was grown in M9 0.4% raffinose, and the culture was split into two flasks when the cells reached mid-log phase. Maleic acid was added to one of the flasks to 20 mM and the cells were incubated for an additional hour. Cells were exposed to 25 mM succinate for the indicated amount of time and the hydrolysis of αPNPG was measured.

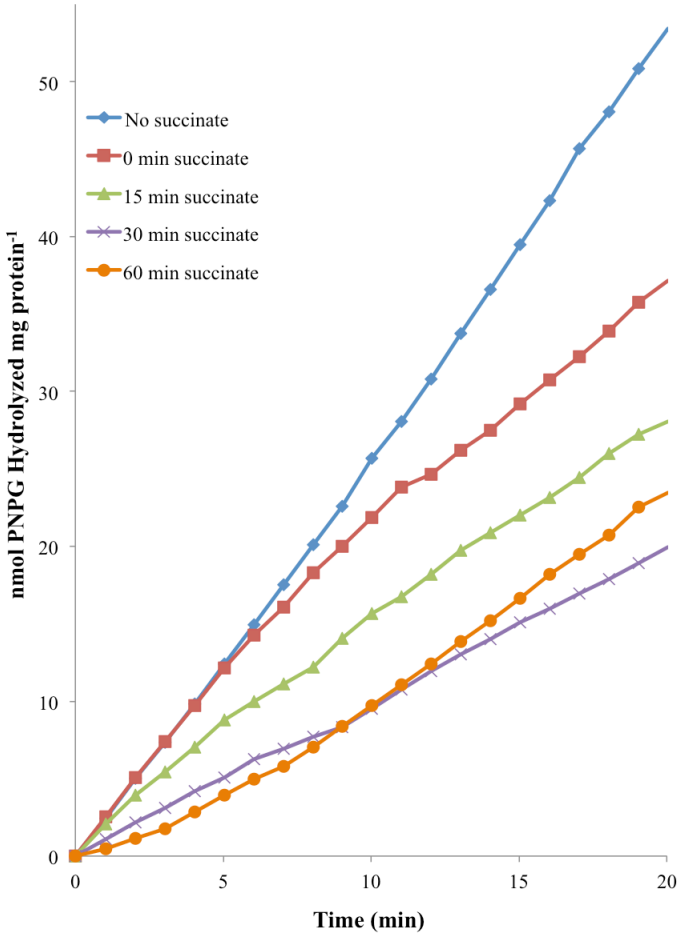

Figure A.8 Kinetic plot of αPNPG hydrolysis. Experiments were the same as in Fig. A.6, graphed as the total amount of αPNPG hydrolyzed in a single experiment instead of hydrolysis rate. Cells were exposed to succinate for the indicated amount of time before addition of 2 mM α-PNPG. Within the first 5 min both succinate-free cells and those exposed to succinate immediately prior to the assay have hydrolyzed the same amount of αPNPG, at which point the hydrolysis rate of succinate exposed cells decreases.

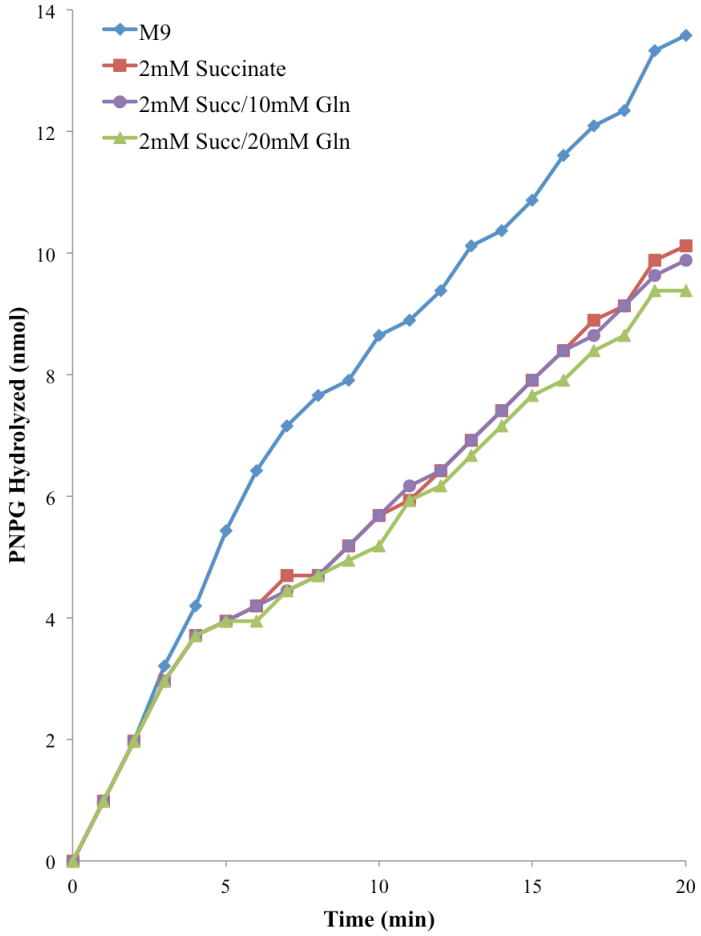

Figure A.9 Hydrolysis of αPNPG in the presence of succinate and glutamine. Washed cells were mixed with glutamine, then succinate. αPNPG was added to 2mM immediately and the rate of *p*-nitrophenol formation was measured by the A_{415}.

References

1. **Vitousek PM, Aber JD, Howarth RW, Likens GE, Matson PA, Schindler DW, Schlesinger WH, Tilman DG.** 1997. Human Alteration of the Global Nitrogen Cycle: Sources and Consequences. Ecol Appl **7:**737-750.
2. **Newton PCD.** 2007. Agroecosystems in a changing climate. CRC/Taylor & Francis, Boca Raton, FL.
3. **Fowler D, Coyle M, Skiba U, Sutton MA, Cape JN, Reis S, Sheppard LJ, Jenkins A, Grizzetti B, Galloway JN, Vitousek P, Leach A, Bouwman AF, Butterbach-Bahl K, Dentener F, Stevenson D, Amann M, Voss M.** 2013. The global nitrogen cycle in the twenty-first century. Philos Trans R Soc Lond B Biol Sci **368:**20130164.
4. **Bouwman L, Goldewijk KK, Van Der Hoek KW, Beusen AH, Van Vuuren DP, Willems J, Rufino MC, Stehfest E.** 2013. Exploring global changes in nitrogen and phosphorus cycles in agriculture induced by livestock production over the 1900-2050 period. Proc Natl Acad Sci U S A **110:**20882-20887.
5. **Erisman JW, Sutton MA, Galloway J, Klimont Z, Winiwarter W.** 2008. How a century of ammonia synthesis changed the world. Nature Geoscience **1:**636-639.
6. **Boddey RM, Alves BJR, Henrique de B. Soares L, Jantalia CP, Urquiaga S.** 2009. Biological Nitrogen Fixation and the Mitigation of Greenhouse Gas Emissions, p 387-413. *In* Emerich DW, Krishnan H (ed), Nitrogen Fixation in Crop Production, vol 52. American Society of Agronomy, Madison, WI.
7. **Galloway JN, Leach AM, Bleeker A, Erisman JW.** 2013. A chronology of human understanding of the nitrogen cycle. Philos Trans R Soc Lond B Biol Sci **368:**20130120.
8. **Burris R.** 2000. Introduction to Nitrogenases, p 33-41. *In* Triplett E (ed), Prokaryotic Nitrogen Fixation: A model system for the analysis of a biological process, 1 ed. Horizon Scientific Press, Madison, WI.
9. **Fisher RF, Long SR.** 1992. Rhizobium-plant signal exchange. Nature **357:**655-660.
10. **Roche P, Maillet F, Plazanet C, Debelle F, Ferro M, Truchet G, Prome JC, Denarie J.** 1996. The common *nodABC* genes of *Rhizobium meliloti* are host-range determinants. Proc Natl Acad Sci U S A **93:**15305-15310.
11. **Jumas-Bilak E, Michaux-Charachon S, Bourg G, Ramuz M, Allardet-Servent A.** 1998. Unconventional genomic organization in the alpha subgroup of the Proteobacteria. J Bacteriol **180:**2749-2755.
12. **Galibert F, Finan TM, Long SR, Puhler A, Abola P, Ampe F, Barloy-Hubler F, Barnett MJ, Becker A, Boistard P, Bothe G, Boutry M, Bowser L, Buhrmester J, Cadieu E, Capela D, Chain P, Cowie A, Davis RW, Dreano S, Federspiel NA, Fisher RF, Gloux S, Godrie T, Goffeau A, Golding B, Gouzy J, Gurjal M, Hernandez-Lucas I, Hong A, Huizar L, Hyman RW, Jones T, Kahn D, Kahn ML, Kalman S, Keating DH, Kiss E, Komp C, Lelaure V, Masuy D, Palm C, Peck MC, Pohl TM, Portetelle D, Purnelle B,**

Ramsperger U, Surzycki R, Thebault P, Vandenbol M, et al. 2001. The composite genome of the legume symbiont *Sinorhizobium meliloti*. Science **293:**668-672.
13. **Batut J, Andersson SGE, O'Callaghan D.** 2004. The evolution of chronic infection strategies in the α-proteobacteria. Nat Rev Microbiol **2:**933-945.
14. **Neal OR, Walker RH.** 1935. Physiological Studies on Rhizobium: IV. Utilization of Carbonaceous Materials. J Bacteriol **30:**173-187.
15. **Dunn MF.** 2014. Key roles of microsymbiont amino acid metabolism in rhizobia-legume interactions. Crit Rev Microbiol doi:10.3109/1040841X.2013.856854.
16. **Gage DJ.** 2004. Infection and invasion of roots by symbiotic, nitrogen-fixing rhizobia during nodulation of temperate legumes. Microbiol Mol Biol Rev **68:**280-300.
17. **Udvardi M, Poole PS.** 2013. Transport and metabolism in legume-rhizobia symbioses. Annu Rev Plant Biol **64:**781-805.
18. **Kuzma MM, Hunt S, Layzell DB.** 1993. Role of Oxygen in the Limitation and Inhibition of Nitrogenase Activity and Respiration Rate in Individual Soybean Nodules. Plant Physiol **101:**161-169.
19. **Pueppke SG, Broughton WJ.** 1999. *Rhizobium* sp. strain NGR234 and *R. fredii* USDA257 share exceptionally broad, nested, host ranges. Mol Plant Microbe Interact **12:**293-318.
20. **Simsek S, Wood K, Reuhs BL.** 2013. Structural analysis of succinoglycan oligosaccharides from *Sinorhizobium meliloti* strains with different host compatibility phenotypes. J Bacteriol **195:**2032-2038.
21. **Oldroyd GE, Murray JD, Poole PS, Downie JA.** 2011. The rules of engagement in the legume-rhizobial symbiosis. Annu Rev Genet **45:**119-144.
22. **Haag AF, Arnold MF, Myka KK, Kerscher B, Dall'Angelo S, Zanda M, Mergaert P, Ferguson GP.** 2013. Molecular insights into bacteroid development during Rhizobium-legume symbiosis. FEMS Microbiol Rev **37:**364-383.
23. **Mendes R, Kruijt M, de Bruijn I, Dekkers E, van der Voort M, Schneider JH, Piceno YM, DeSantis TZ, Andersen GL, Bakker PA, Raaijmakers JM.** 2011. Deciphering the rhizosphere microbiome for disease-suppressive bacteria. Science **332:**1097-1100.
24. **Dakora FD, Phillips DA.** 2002. Root exudates as mediators of mineral acquisition in low-nutrient environments. Plant and Soil **245:**35-47.
25. **Hartwig UA, Joseph CM, Phillips DA.** 1991. Flavonoids Released Naturally from Alfalfa Seeds Enhance Growth Rate of *Rhizobium meliloti*. Plant Physiol **95:**797-803.
26. **Cook RJ, Thomashow LS, Weller DM, Fujimoto D, Mazzola M, Bangera G, Kim DS.** 1995. Molecular mechanisms of defense by rhizobacteria against root disease. Proc Natl Acad Sci U S A **92:**4197-4201.
27. **Glucksman E, Bell T, Griffiths RI, Bass D.** 2010. Closely related protist strains have different grazing impacts on natural bacterial communities. Environ Microbiol **12:**3105-3113.

28. **Li DM, Alexander M.** 1986. Bacterial growth rates and competition affect nodulation and root colonization by *Rhizobium meliloti*. Appl Environ Microbiol **52:**807-811.
29. **Mnasri B, Aouani ME, Mhamdi R.** 2007. Nodulation and growth of common bean (*Phaseolus vulgaris*) under water deficiency. Soil Biol Biochem **39:**1744-1750.
30. **Mendes IC, Bottomley PJ.** 1998. Distribution of a Population of *Rhizobium leguminosarum* bv. trifolii among Different Size Classes of Soil Aggregates. Appl Environ Microbiol **64:**970-975.
31. **Yang SS, Bellogin RA, Buendia A, Camacho M, Chen M, Cubo T, Daza A, Diaz CL, Espuny MR, Gutierrez R, Harteveld M, Li XH, Lyra MC, Madinabeitia N, Medina C, Miao L, Ollero FJ, Olsthoorn MM, Rodriguez DN, Santamaria C, Schlaman HR, Spaink HP, Temprano F, Thomas-Oates JE, Van Brussel AA, Vinardell JM, Xie F, Yang J, Zhang HY, Zhen J, Zhou J, Ruiz-Sainz JE.** 2001. Effect of pH and soybean cultivars on the quantitative analyses of soybean rhizobia populations. J Biotechnol **91:**243-255.
32. **Graham PH.** 1992. Stress tolerance in *Rhizobium* and *Bradyrhizobium*, and nodulation under adverse soil conditions. Can J Microbiol **38:**475-484.
33. **Tesfaye M.** 2003. Influence of enhanced malate dehydrogenase expression by alfalfa on diversity of rhizobacteria and soil nutrient availability. Soil Biol Biochem **35:**1103-1113.
34. **Jones DL, Clode PL, Kilburn MR, Stockdale EA, Murphy DV.** 2013. Competition between plant and bacterial cells at the microscale regulates the dynamics of nitrogen acquisition in wheat (*Triticum aestivum*). New Phytol **200:**796-807.
35. **Frazier WC, Fred EB.** 1922. Movement of legume bacteria in soil. Soil Sci **14:**29-36.
36. **McDermott TR, Graham PH.** 1989. *Bradyrhizobium japonicum* Inoculant Mobility, Nodule Occupancy, and Acetylene Reduction in the Soybean Root System. Appl Environ Microbiol **55:**2493-2498.
37. **Day DA, Carroll BJ, Delves AC, Gresshoff PM.** 1989. Relationship between autoregulation and nitrate inhibition of nodulation in soybeans. Physiologia Plantarum **75:**37-42.
38. **Elise S, Etienne-Pascal J, de Fernanda C-N, Gérard D, Julia F.** 2005. The *Medicago truncatula SUNN* Gene Encodes a CLV1-like Leucine-rich Repeat Receptor Kinase that Regulates Nodule Number and Root Length. Plant Mol Biol **58:**809-822.
39. **Magori S, Oka-Kira E, Shibata S, Umehara Y, Kouchi H, Hase Y, Tanaka A, Sato S, Tabata S, Kawaguchi M.** 2009. *TOO MUCH LOVE*, a Root Regulator Associated with the Long-Distance Control of Nodulation in *Lotus japonicus*. Mol Plant Microbe Interact **22:**259-268.
40. **Oono R, Anderson CG, Denison RF.** 2011. Failure to fix nitrogen by non-reproductive symbiotic rhizobia triggers host sanctions that reduce fitness of their reproductive clonemates. Proc R Soc Lond B Biol Sci **278:**2698-2703.
41. **Kiers ET, Rousseau RA, West SA, Denison RF.** 2003. Host sanctions and the legume-rhizobium mutualism. Nature **425:**78-81.

42. **Mulligan JT, Long SR.** 1989. A family of activator genes regulates expression of *Rhizobium meliloti* nodulation genes. Genetics **122:**7-18.
43. **Oldroyd GE.** 2013. Speak, friend, and enter: signalling systems that promote beneficial symbiotic associations in plants. Nat Rev Microbiol **11:**252-263.
44. **Cooper JE.** 2007. Early interactions between legumes and rhizobia: disclosing complexity in a molecular dialogue. J Appl Microbiol **103:**1355-1365.
45. **D'Haeze W, Holsters M.** 2002. Nod factor structures, responses and perception during initiation of nodule development. Glycobiology **12:**79R-105R.
46. **Ridge RW, Rolfe BG.** 1985. Rhizobium sp. Degradation of Legume Root Hair Cell Wall at the Site of Infection Thread Origin. Appl Environ Microbiol **50:**717-720.
47. **Gage DJ.** 2002. Analysis of infection thread development using Gfp- and DsRed-expressing *Sinorhizobium meliloti*. J Bacteriol **184:**7042-7046.
48. **Pellock BJ, Cheng HP, Walker GC.** 2000. Alfalfa root nodule invasion efficiency is dependent on *Sinorhizobium meliloti* polysaccharides. J Bacteriol **182:**4310-4318.
49. **Timmers AC, Auriac MC, Truchet G.** 1999. Refined analysis of early symbiotic steps of the Rhizobium-Medicago interaction in relationship with microtubular cytoskeleton rearrangements. Development **126:**3617-3628.
50. **Mergaert P, Uchiumi T, Alunni B, Evanno G, Cheron A, Catrice O, Mausset AE, Barloy-Hubler F, Galibert F, Kondorosi A, Kondorosi E.** 2006. Eukaryotic control on bacterial cell cycle and differentiation in the Rhizobium-legume symbiosis. Proc Natl Acad Sci U S A **103:**5230-5235.
51. **Ott T, van Dongen JT, Gunther C, Krusell L, Desbrosses G, Vigeolas H, Bock V, Czechowski T, Geigenberger P, Udvardi MK.** 2005. Symbiotic leghemoglobins are crucial for nitrogen fixation in legume root nodules but not for general plant growth and development. Curr Biol **15:**531-535.
52. **Preisig O, Zufferey R, Thony-Meyer L, Appleby CA, Hennecke H.** 1996. A high-affinity cbb_3-type cytochrome oxidase terminates the symbiosis-specific respiratory chain of *Bradyrhizobium japonicum*. J Bacteriol **178:**1532-1538.
53. **Engelke T, Jording D, Kapp D, Puhler A.** 1989. Identification and sequence analysis of the *Rhizobium meliloti dctA* gene encoding the C_4-dicarboxylate carrier. J Bacteriol **171:**5551-5560.
54. **Yurgel SN, Kahn ML.** 2004. Dicarboxylate transport by rhizobia. FEMS Microbiol Rev **28:**489-501.
55. **Geddes BA, Oresnik IJ.** 2014. Physiology, genetics, and biochemistry of carbon metabolism in the alphaproteobacterium *Sinorhizobium meliloti*. Can J Microbiol **60:**491-507.
56. **Osteras M, Driscoll BT, Finan TM.** 1997. Increased pyruvate orthophosphate dikinase activity results in an alternative gluconeogenic pathway in *Rhizobium* (*Sinorhizobium*) *meliloti*. Microbiology **143 (Pt 5):**1639-1648.

57. **Finan TM, McWhinnie E, Driscoll B, Watson RJ.** 1991. Complex Symbiotic Phenotypes Result from Gluconeogenic Mutations in *Rhizobium meliloti*. Mol Plant Microbe Interact **4:**386.
58. **Driscoll BT, Finan TM.** 1993. NAD(+)-dependent malic enzyme of *Rhizobium meliloti* is required for symbiotic nitrogen fixation. Mol Microbiol **7:**865-873.
59. **Osteraas M, O'Brien SAP, Finan TM.** 1997. Genetic analysis of mutations affecting *pckA* regulation in *Rhizobium (Sinorhizobium) meliloti*. Genetics **147:**1521-1531.
60. **Trainer MA, Charles TC.** 2006. The role of PHB metabolism in the symbiosis of rhizobia with legumes. Appl Microbiol Biotechnol **71:**377-386.
61. **Wang C, Saldanha M, Sheng X, Shelswell KJ, Walsh KT, Sobral BW, Charles TC.** 2007. Roles of poly-3-hydroxybutyrate (PHB) and glycogen in symbiosis of *Sinorhizobium meliloti* with *Medicago* sp. Microbiology **153:**388-398.
62. **Patriarca EJ, Tate R, Iaccarino M.** 2002. Key role of bacterial NH_4^+ metabolism in Rhizobium-plant symbiosis. Microbiol Mol Biol Rev **66:**203-222.
63. **Sanchez F, Padilla JE, Perez H, Lara M.** 1991. Control of Nodulin Genes in Root-Nodule Development and Metabolism. Annu Rev Plant Physiol Plant Mol Biol **42:**507-528.
64. **Dam S, Dyrlund TF, Ussatjuk A, Jochimsen B, Nielsen K, Goffard N, Ventosa M, Lorentzen A, Gupta V, Andersen SU, Enghild JJ, Ronson CW, Roepstorff P, Stougaard J.** 2014. Proteome reference maps of the *Lotus japonicus* nodule and root. Proteomics **14:**230-240.
65. **Dos Santos PC, Fang Z, Mason SW, Setubal JC, Dixon R.** 2012. Distribution of nitrogen fixation and nitrogenase-like sequences amongst microbial genomes. BMC Genomics **13:**162.
66. **Dixon R, Kahn D.** 2004. Genetic regulation of biological nitrogen fixation. Nat Rev Microbiol **2:**621-631.
67. **Barnett MJ, Fisher RF.** 2006. Global gene expression in the rhizobium-legume symbiosis. Symbiosis **42:**1-24.
68. **Bush M, Dixon R.** 2012. The role of bacterial enhancer binding proteins as specialized activators of σ^{54}-dependent transcription. Microbiol Mol Biol Rev **76:**497-529.
69. **McGlynn SE, Boyd ES, Peters JW, Orphan VJ.** 2012. Classifying the metal dependence of uncharacterized nitrogenases. Front Microbiol **3:**419.
70. **Hoffman BM, Lukoyanov D, Yang ZY, Dean DR, Seefeldt LC.** 2014. Mechanism of nitrogen fixation by nitrogenase: the next stage. Chem Rev **114:**4041-4062.
71. **Soga T.** 2013. Cancer metabolism: key players in metabolic reprogramming. Cancer Sci **104:**275-281.
72. **Salminen A, Kaarniranta K, Hiltunen M, Kauppinen A.** 2014. Krebs cycle dysfunction shapes epigenetic landscape of chromatin: Novel insights into mitochondrial regulation of aging process. Cell Signal **26:**1598-1603.

73. **Yu Y, Clippinger AJ, Alwine JC.** 2011. Viral effects on metabolism: changes in glucose and glutamine utilization during human cytomegalovirus infection. Trends Microbiol **19:**360-367.
74. **Rodriguez-Gallego E, Guirro M, Riera-Borrull M, Hernandez-Aguilera A, Marine-Casado R, Fernandez-Arroyo S, Beltran-Debon R, Sabench F, Hernandez M, Del Castillo D, Menendez JA, Camps J, Ras R, Arola L, Joven J.** 2015. Mapping of the circulating metabolome reveals α-ketoglutarate as a predictor of morbid obesity-associated non-alcoholic fatty liver disease. Int J Obes (Lond) **39:**279-287.
75. **Hou Y, Wang L, Ding B, Liu Y, Zhu H, Liu J, Li Y, Kang P, Yin Y, Wu G.** 2011. Alpha-Ketoglutarate and intestinal function. Front Biosci (Landmark Ed) **16:**1186-1196.
76. **Dunn MF, Ramirez-Trujillo JA, Hernandez-Lucas I.** 2009. Major roles of isocitrate lyase and malate synthase in bacterial and fungal pathogenesis. Microbiology **155:**3166-3175.
77. **Eisenreich W, Dandekar T, Heesemann J, Goebel W.** 2010. Carbon metabolism of intracellular bacterial pathogens and possible links to virulence. Nat Rev Microbiol **8:**401-412.
78. **Zhang L, Chiang WC, Gao Q, Givskov M, Tolker-Nielsen T, Yang L, Zhang G.** 2012. The catabolite repression control protein Crc plays a role in the development of antimicrobial-tolerant subpopulations in *Pseudomonas aeruginosa* biofilms. Microbiology **158:**3014-3019.
79. **Kern A, Tilley E, Hunter IS, Legisa M, Glieder A.** 2007. Engineering primary metabolic pathways of industrial micro-organisms. J Biotechnol **129:**6-29.
80. **Tsuji A, Okada S, Hols P, Satoh E.** 2013. Metabolic engineering of *Lactobacillus plantarum* for succinic acid production through activation of the reductive branch of the tricarboxylic acid cycle. Enzyme Microb Technol **53:**97-103.
81. **Rossouw D, Heyns EH, Setati ME, Bosch S, Bauer FF.** 2013. Adjustment of trehalose metabolism in wine *Saccharomyces cerevisiae* strains to modify ethanol yields. Appl Environ Microbiol **79:**5197-5207.
82. **Studer SV, Mandel MJ, Ruby EG.** 2008. AinS quorum sensing regulates the *Vibrio fischeri* acetate switch. J Bacteriol **190:**5915-5923.
83. **Prell J, Poole P.** 2006. Metabolic changes of rhizobia in legume nodules. Trends Microbiol **14:**161-168.
84. **Morange M.** 2006. What history tells us V. Emile Duclaux (1840-1904). J Biosci **31:**215-218.
85. **Kundig W, Ghosh S, Roseman S.** 1964. Phosphate bound to histidine in a protein as an intermediate in a novel phospho-transferase system. Proc Natl Acad Sci U S A **52:**1067-1074.
86. **Saier MH, Roseman S.** 1972. Inducer exclusion and repression of enzyme synthesis in mutants of *Salmonella typhimurium* defective in enzyme I of the phosphoenolpyruvate: sugar phosphotransferase system. J Biol Chem **247:**972-975.

87. **Deutscher J, Francke C, Postma PW.** 2006. How phosphotransferase system-related protein phosphorylation regulates carbohydrate metabolism in bacteria. Micro Mol Biol Rev **70:**939-1031.
88. **Kundig W, Roseman S.** 1971. Sugar transport. II. Characterization of constitutive membrane-bound enzymes II of the *Escherichia coli* phosphotransferase system. J Biol Chem **246:**1407-1418.
89. **Weigel N, Kukuruzinska MA, Nakazawa A, Waygood EB, Roseman S.** 1982. Sugar transport by the bacterial phosphotransferase system. Phosphoryl transfer reactions catalyzed by enzyme I of *Salmonella typhimurium*. J Biol Chem **257:**14477-14491.
90. **Saier MH, Jr., Feucht BU, Hofstadter LJ.** 1976. Regulation of carbohydrate uptake and adenylate cyclase activity mediated by the enzymes II of the phosphoenolpyruvate: sugar phosphotransferase system in *Escherichia coli*. J Biol Chem **251:**883-892.
91. **Deutscher J, Saier MH, Jr.** 1983. ATP-dependent protein kinase-catalyzed phosphorylation of a seryl residue in HPr, a phosphate carrier protein of the phosphotransferase system in *Streptococcus pyogenes*. Proc Natl Acad Sci U S A **80:**6790-6794.
92. **Deutscher J, Kuster E, Bergstedt U, Charrier V, Hillen W.** 1995. Protein kinase-dependent HPr/CcpA interaction links glycolytic activity to carbon catabolite repression in gram-positive bacteria. Mol Microbiol **15:**1049-1053.
93. **Ramstrom H, Sanglier S, Leize-Wagner E, Philippe C, Van Dorsselaer A, Haiech J.** 2003. Properties and regulation of the bifunctional enzyme HPr kinase/phosphatase in *Bacillus subtilis*. J Biol Chem **278:**1174-1185.
94. **Barabote RD, Saier MH, Jr.** 2005. Comparative genomic analyses of the bacterial phosphotransferase system. Microbiol Mol Biol Rev **69:**608-634.
95. **Reizer J, Reizer A, Merrick MJ, Plunkett G, 3rd, Rose DJ, Saier MH, Jr.** 1996. Novel phosphotransferase-encoding genes revealed by analysis of the *Escherichia coli* genome: a chimeric gene encoding an Enzyme I homologue that possesses a putative sensory transduction domain. Gene **181:**103-108.
96. **Lee CR, Cho SH, Yoon MJ, Peterkofsky A, Seok YJ.** 2007. *Escherichia coli* enzyme IIA^{Ntr} regulates the K^+ transporter TrkA. Proc Natl Acad Sci U S A **104:**4124-4129.
97. **Luttmann D, Heermann R, Zimmer B, Hillmann A, Rampp IS, Jung K, Gorke B.** 2009. Stimulation of the potassium sensor KdpD kinase activity by interaction with the phosphotransferase protein IIA^{Ntr} in *Escherichia coli*. Mol Microbiol **72:**978-994.
98. **Lee CR, Cho SH, Kim HJ, Kim M, Peterkofsky A, Seok YJ.** 2010. Potassium mediates *Escherichia coli* enzyme IIA^{Ntr} -dependent regulation of sigma factor selectivity. Mol Microbiol **78:**1468-1483.
99. **Luttmann D, Gopel Y, Gorke B.** 2012. The phosphotransferase protein $EIIA^{Ntr}$ modulates the phosphate starvation response through interaction with histidine kinase PhoR in *Escherichia coli*. Mol Microbiol **86:**96-110.
100. **Jahn S, Haverkorn van Rijsewijk BR, Sauer U, Bettenbrock K.** 2013. A role for $EIIA^{Ntr}$ in controlling fluxes in the central metabolism of *E. coli* K12. Biochim Biophys Acta **1833:**2879-2889.

101. **Karstens K, Zschiedrich CP, Bowien B, Stulke J, Gorke B.** 2014. Phosphotransferase protein EIIA^{Ntr} interacts with SpoT, a key enzyme of the stringent response, in *Ralstonia eutropha* H16. Microbiology **160:**711-722.
102. **Ucker DS.** 1978. Catabolite repression-like phenomenon in *Rhizobium meliloti*. J Bacteriol **136:**1197-1200.
103. **George SE, Costenbader CJ, Melton T.** 1985. Diauxic growth in *Azotobacter vinelandii*. J Bacteriol **164:**866-871.
104. **Mukherjee A, Ghosh S.** 1987. Regulation of fructose uptake and catabolism by succinate in *Azospirillum brasilense*. J Bacteriol **169:**4361-4367.
105. **de Vries GE, van Brussel AA, Quispel A.** 1982. Mechanism of regulation of glucose transport in *Rhizobium leguminosarum*. J Bacteriol **149:**872-879.
106. **Valentini M, Garcia-Maurino SM, Perez-Martinez I, Santero E, Canosa I, Lapouge K.** 2014. Hierarchical management of carbon sources is regulated similarly by the CbrA/B systems in *Pseudomonas aeruginosa* and *Pseudomonas putida*. Microbiology **160:**2243-2252.
107. **Gage DJ, Long SR.** 1998. α-galactoside uptake in *Rhizobium meliloti*: isolation and characterization of *agpA*, a gene encoding a periplasmic binding protein required for melibiose and raffinose utilization. J Bacteriol **180:**5739-5748.
108. **Bringhurst RM, Gage DJ.** 2000. An AraC-like transcriptional activator is required for induction of genes needed for α-galactoside utilization in *Sinorhizobium meliloti*. FEMS Microbiol Letters **188:**23-27.
109. **Bringhurst RM, Gage DJ.** 2002. Control of inducer accumulation plays a key role in succinate-mediated catabolite repression in *Sinorhizobium meliloti*. J Bacteriol **184:**5385-5392.
110. **Arango-Pinedo C, Bringhurst RM, Gage DJ.** 2008. *Sinorhizobium meliloti* mutants lacking phosphotransferase system enzyme HPr or EIIA are altered in diverse processes, including carbon metabolism, cobalt requirements, and succinoglycan production. J Bacteriol **190:**2947-2956.
111. **Pinedo CA, Gage DJ.** 2009. HPrK regulates succinate-mediated catabolite repression in the gram-negative symbiont *Sinorhizobium meliloti*. J Bacteriol **191:**298-309.
112. **Dozot M, Poncet S, Nicolas C, Copin R, Bouraoui H, Maze A, Deutscher J, De Bolle X, Letesson JJ.** 2010. Functional characterization of the incomplete phosphotransferase system (PTS) of the intracellular pathogen *Brucella melitensis*. PLoS One **5**.
113. **Garcia PP, Bringhurst RM, Arango Pinedo C, Gage DJ.** 2010. Characterization of a two-component regulatory system that regulates succinate-mediated catabolite repression in *Sinorhizobium meliloti*. J Bacteriol **192:**5725-5735.
114. **Sheftic SR, Garcia PP, White E, Robinson VL, Gage DJ, Alexandrescu AT.** 2012. Nuclear magnetic resonance structure and dynamics of the response regulator Sma0114 from *Sinorhizobium meliloti*. Biochemistry **51:**6932-6941.
115. **Studier FW.** 2005. Protein production by auto-induction in high density shaking cultures. Protein Expr Purif **41:**207-234.

116. **Warrens AN, Jones MD, Lechler RI.** 1997. Splicing by overlap extension by PCR using asymmetric amplification: an improved technique for the generation of hybrid proteins of immunological interest. Gene **186:**29-35.
117. **Mclellan T.** 1982. Electrophoresis Buffers for Polyacrylamide Gels at Various pH. Anal Biochem **126:**94-99.
118. **Waygood EB, Meadow ND, Roseman S.** 1979. Modified Assay Procedures for the Phosphotransferase System in Enteric Bacteria. Anal Biochem **95:**293-304.
119. **Casabon I, Couture M, Vaillancourt K, Vadeboncoeur C.** 2009. Kinetic Studies of HPr, HPr(H15D), HPr(H15E), and HPr(His~P) Phosphorylation by the *Streptococcus salivarius* HPr(Ser) Kinase/Phosphorylase. Biochemistry **48:**10765-10774.
120. **Meade HM, Long SR, Ruvkun GB, Brown SE, Ausubel FM.** 1982. Physical and genetic characterization of symbiotic and auxotrophic mutants of *Rhizobium meliloti* induced by transposon Tn*5* mutagenesis. J Bacteriol **149:**114-122.
121. **Goodwin RA, Gage DJ.** 2014. Biochemical characterization of a nitrogen-type phosphotransferase system reveals that enzyme EI^{Ntr} integrates carbon and nitrogen signaling in *Sinorhizobium meliloti*. J Bacteriol **196:**1901-1907.
122. **LiCalsi C, Crocenzi TS, Freire E, Roseman S.** 1991. Sugar transport by the bacterial phosphotransferase system. Structural and thermodynamic domains of enzyme I of *Salmonella typhimurium*. J Biol Chem **266:**19519-19527.
123. **Kukuruzinska MA, Turner BW, Ackers GK, Roseman S.** 1984. Subunit association of enzyme I of the *Salmonella typhimurium* phosphoenolpyruvate: glycose phosphotransferase system. Temperature dependence and thermodynamic properties. J Biol Chem **259:**11679-11681.
124. **Weigel N, Waygood EB, Kukuruzinska MA, Nakazawa A, Roseman S.** 1982. Sugar transport by the bacterial phosphotransferase system. Isolation and characterization of enzyme I from *Salmonella typhimurium*. J Biol Chem **257:**14461-14469.
125. **Meadow ND, Mattoo RL, Savtchenko RS, Roseman S.** 2005. Transient state kinetics of Enzyme I of the phosphoenolpyruvate:glycose phosphotransferase system of *Escherichia coli*: Equilibrium and second-order rate constants for the phosphotransfer reactions with phosphoenolpyruvate and HPr. Biochemistry **44:**12790-12796.
126. **Casabon I, Couture M, Vaillancourt K, Vadeboncoeur C.** 2006. Synthesis of HPr(Ser-P)(His~P) by enzyme I of the phosphoenolpyruvate:sugar phosphotransferase system of *Streptococcus salivarius*. Biochemistry **45:**6692-6702.
127. **Doucette CD, Schwab DJ, Wingreen NS, Rabinowitz JD.** 2011. α-Ketoglutarate coordinates carbon and nitrogen utilization via enzyme I inhibition. Nat Chem Biol **7:**894-901.
128. **Chubukov V, Gerosa L, Kochanowski K, Sauer U.** 2014. Coordination of microbial metabolism. Nat Rev Microbiol **12:**327-340.

129. **You C, Okano H, Hui S, Zhang Z, Kim M, Gunderson CW, Wang YP, Lenz P, Yan D, Hwa T.** 2013. Coordination of bacterial proteome with metabolism by cyclic AMP signalling. Nature **500:**301-306.
130. **Peterkofsky A, Wang G, Seok Y-J.** 2006. Parallel PTS systems. Arch Biochem Biophys **453:**101.
131. **Lee CR, Park YH, Kim M, Kim YR, Park S, Peterkofsky A, Seok YJ.** 2013. Reciprocal regulation of the autophosphorylation of enzyme I^{Ntr} by glutamine and alpha-ketoglutarate in *Escherichia coli*. Mol Microbiol **88:**473-485.
132. **Rabus R, Reizer J, Paulsen I, Saier MH.** 1999. Enzyme I^{Ntr} from *Escherichia coli* - A novel enzyme of the phosphoenolpyruvate-dependent phosphotransferase system exhibiting strict specificity for its phosphoryl acceptor, NPr. J Biol Chem **274:**26185-26191.
133. **Piszczek G, Lee JC, Tjandra N, Lee CR, Seok YJ, Levine RL, Peterkofsky A.** 2011. Deuteration of *Escherichia coli* enzyme I^{Ntr} alters its stability. Arch Biochem Biophys **507:**332-342.
134. **King ND, O'Brian MR.** 2001. Evidence for direct interaction between enzyme I^{Ntr} and aspartokinase to regulate bacterial oligopeptide transport. J Biol Chem **276:**21311-21316.
135. **Aravind L, Ponting CP.** 1997. The GAF domain: an evolutionary link between diverse phototransducing proteins. Trends Biochem Sci **22:**458-459.
136. **Yoshimitsu K, Takatani N, Miura Y, Watanabe Y, Nakajima H.** 2011. The role of the GAF and central domains of the transcriptional activator VnfA in *Azotobacter vinelandii*. Febs Journal **278:**3287-3297.
137. **Little R, Dixon R.** 2003. The amino-terminal GAF domain of *Azotobacter vinelandii* NifA binds 2-oxoglutarate to resist inhibition by NifL under nitrogen-limiting conditions. J Biol Chem **278:**28711-28718.
138. **van Heeswijk WC, Westerhoff HV, Boogerd FC.** 2013. Nitrogen assimilation in *Escherichia coli*: putting molecular data into a systems perspective. Microbiol Mol Biol Rev **77:**628-695.
139. **Szeto WW, Nixon BT, Ronson CW, Ausubel FM.** 1987. Identification and characterization of the *Rhizobium meliloti ntrC* gene: *R. meliloti* has separate regulatory pathways for activation of nitrogen fixation genes in free-living and symbiotic cells. J Bacteriol **169:**1423-1432.
140. **Davalos M, Fourment J, Lucas A, Berges H, Kahn D.** 2004. Nitrogen regulation in *Sinorhizobium meliloti* probed with whole genome arrays. FEMS Microbiol Lett **241:**33-40.
141. **Yurgel SN, Kahn ML.** 2008. A mutant GlnD nitrogen sensor protein leads to a nitrogen-fixing but ineffective *Sinorhizobium meliloti* symbiosis with alfalfa. Proc Nat Acad Sci**:**18958 –18963.
142. **Yurgel SN, Rice J, Kahn ML.** 2012. Nitrogen metabolism in *Sinorhizobium meliloti*-alfalfa symbiosis: dissecting the role of GlnD and PII proteins. Mol Plant Microbe Interact **25:**355-362.
143. **Shatters RG, Liu Y, Kahn ML.** 1993. Isolation and characterization of a novel glutamine synthetase from *Rhizobium meliloti*. J Biol Chem **268:**469-475.

144. **Yurgel SN, Rice J, Mulder M, Kahn ML.** 2010. GlnB/GlnK PII proteins and regulation of the *Sinorhizobium meliloti* Rm1021 nitrogen stress response and symbiotic function. J Bacteriol **192:**2473-2481.
145. **Arcondeguy T, Huez I, Tillard P, Gangneux C, de Billy F, Gojon A, Truchet G, Kahn D.** 1997. The *Rhizobium meliloti* PII protein, which controls bacterial nitrogen metabolism, affects alfalfa nodule development. Genes Dev **11:**1194-1206.
146. **Gruswitz F, O'Connell J, 3rd, Stroud RM.** 2007. Inhibitory complex of the transmembrane ammonia channel, AmtB, and the cytosolic regulatory protein, GlnK, at 1.96 A. Proc Natl Acad Sci U S A **104:**42-47.
147. **Ho YS, Burden LM, Hurley JH.** 2000. Structure of the GAF domain, a ubiquitous signaling motif and a new class of cyclic GMP receptor. EMBO J **19:**5288-5299.
148. **Gonzalez CF, Stonestrom AJ, Lorca GL, Saier MH, Jr.** 2005. Biochemical characterization of phosphoryl transfer involving HPr of the phosphoenolpyruvate-dependent phosphotransferase system in *Treponema denticola*, an organism that lacks PTS permeases. Biochemistry **44:**598-608.
149. **Untiet V, Karunakaran R, Kramer M, Poole P, Priefer U, Prell J.** 2013. ABC transport is inactivated by the PTS^{Ntr} under potassium limitation in *Rhizobium leguminosarum* 3841. PLoS One **8:**e64682.
150. **Bettenbrock K, Sauter T, Jahreis K, Kremling A, Lengeler JW, Gilles ED.** 2007. Correlation between growth rates, $EIIA^{Crr}$ phosphorylation, and intracellular cyclic AMP levels in *Escherichia coli* K-12. J Bacteriol **189:**6891-6900.
151. **Bennett BD, Kimball EH, Gao M, Osterhout R, Van Dien SJ, Rabinowitz JD.** 2009. Absolute metabolite concentrations and implied enzyme active site occupancy in *Escherichia coli*. Nat Chem Biol **5:**593-599.
152. **Hogema BM, Arents JC, Bader R, Eijkemans K, Yoshida H, Takahashi H, Aiba H, Postma PW.** 1998. Inducer exclusion in *Escherichia coli* by non-PTS substrates: the role of the PEP to pyruvate ratio in determining the phosphorylation state of enzyme IIA^{Glc}. Mol Microbiol **30:**487-498.
153. **Azuaga AI, Neira JL, van Nuland NA.** 2005. HPr as a model protein in structure, interaction, folding and stability studies. Protein Pept Lett **12:**123-137.
154. **Jia Z, Quail JW, Waygood EB, Delbaere LT.** 1993. The 2.0-Å resolution structure of *Escherichia coli* histidine-containing phosphocarrier protein HPr. A redetermination. J Biol Chem **268:**22490-22501.
155. **Anderson JW, Pullen K, Georges F, Klevit RE, Waygood EB.** 1993. The Involvement of the Arginine-17 Residue in the Active-Site of the Histidine-Containing Protein, Hpr, of the Phosphoenolpyruvate - Sugar Phosphotransferase System of *Escherichia coli*. J Biol Chem **268:**12325-12333.
156. **Seok YJ, Sondej M, Badawi P, Lewis MS, Briggs MC, Jaffe H, Peterkofsky A.** 1997. High affinity binding and allosteric regulation of *Escherichia coli* glycogen phosphorylase by the histidine phosphocarrier protein, HPr. J Biol Chem **272:**26511-26521.

157. **Park YH, Lee CR, Choe M, Seok YJ.** 2013. HPr antagonizes the anti-σ^{70} activity of Rsd in *Escherichia coli*. Proc Natl Acad Sci U S A **110:**21142-21147.
158. **Kim HM, Park YH, Yoon CK, Seok YJ.** 2015. Histidine phosphocarrier protein regulates pyruvate kinase A activity in response to glucose in *Vibrio vulnificus*. Mol Microbiol doi:10.1111/mmi.12936.
159. **Attwood PV, Piggott MJ, Zu XL, Besant PG.** 2007. Focus on phosphohistidine. Amino Acids **32:**145-156.
160. **Stock JB, Stock AM, Mottonen JM.** 1990. Signal transduction in bacteria. Nature **344:**395-400.
161. **Duclos B, Marcandier S, Cozzone AJ.** 1991. Chemical properties and separation of phosphoamino acids by thin-layer chromatography and/or electrophoresis. Methods Enzymol **201:**10-21.
162. **Anderson B, Weigel N, Kundig W, Roseman S.** 1971. Sugar transport. III. Purification and properties of a phosphocarrier protein (HPr) of the phosphoenolpyruvate-dependent phosphotransferase system of *Escherichia coli*. J Biol Chem **246:**7023-7033.
163. **Waygood EB, Erickson E, el Kabbani OA, Delbaere LT.** 1985. Characterization of phosphorylated histidine-containing protein (HPr) of the bacterial phosphoenolpyruvate:sugar phosphotransferase system. Biochemistry **24:**6938-6945.
164. **Hultquist DE.** 1968. The preparation and characterization of phosphorylated derivatives of histidine. Biochim Biophys Acta **153:**329-340.
165. **Simoni RD, Hays JB, Nakazawa T, Roseman S.** 1973. Sugar transport. VI. Phosphoryl transfer in the lactose phosphotransferase system of *Staphylococcus aureus*. J Biol Chem **248:**957-965.
166. **Waygood EB, Pasloske K, Delbaere LT, Deutscher J, Hengstenberg W.** 1988. Characterization of the 1-phosphohistidinyl residue in the phosphocarrier protein HPr of the phosphoenolpyruvate: sugar phosphotransferase system of *Streptococcus faecalis*. Biochem Cell Biol **66:**76-80.
167. **Anderson JW, Bhanot P, Georges F, Klevit RE, Waygood EB.** 1991. Involvement of the carboxy-terminal residue in the active site of the histidine-containing protein, HPr, of the phosphoenolpyruvate:sugar phosphotransferase system of *Escherichia coli*. Biochemistry **30:**9601-9607.
168. **Koch S, Sutrina SL, Wu LF, Reizer J, Schnetz K, Rak B, Saier MH, Jr.** 1996. Identification of a site in the phosphocarrier protein, HPr, which influences its interactions with sugar permeases of the bacterial phosphotransferase system: kinetic analyses employing site-specific mutants. J Bacteriol **178:**1126-1133.
169. **Cases I, Velazquez F, de Lorenzo V.** 2007. The ancestral role of the phosphoenolpyruvate-carbohydrate phosphotransferase system (PTS) as exposed by comparative genomics. Res Microbiol **158:**666-670.
170. **Meza E, Becker J, Bolivar F, Gosset G, Wittmann C.** 2012. Consequences of phosphoenolpyruvate:sugar phosphotranferase system and pyruvate kinase

isozymes inactivation in central carbon metabolism flux distribution in *Escherichia coli*. Microb Cell Fact **11:**127.

171. **Halbedel S, Busse J, Schmidl SR, Stulke J.** 2006. Regulatory protein phosphorylation in *Mycoplasma pneumoniae*. A PP2C-type phosphatase serves to dephosphorylate HPr(Ser-P). J Biol Chem **281:**26253-26259.
172. **Kelley LA, Sternberg MJ.** 2009. Protein structure prediction on the Web: a case study using the Phyre server. Nat Protoc **4:**363-371.
173. **Yurgel S, Mortimer MW, Rogers KN, Kahn ML.** 2000. New substrates for the dicarboxylate transport system of *Sinorhizobium meliloti*. J Bacteriol **182:**4216-4221.